

# A Review on Organ Deformation Modeling Approaches for Reliable Surgical Navigation using Augmented Reality

Zheng Han and Qi Dou

Department of Computer Science and Engineering, The Chinese University of Hong Kong, Hong Kong, China

## ABSTRACT

Augmented Reality (AR) holds the potential to revolutionize surgical procedures by allowing surgeons to visualize critical structures within the patient's body. This is achieved through superimposing preoperative organ models onto the actual anatomy. Challenges arise from dynamic deformations of organs during surgery, making preoperative models inadequate for faithfully representing intraoperative anatomy. To enable reliable navigation in augmented surgery, modeling of intraoperative deformation to obtain an accurate alignment of the preoperative organ model with the intraoperative anatomy is indispensable. Despite the existence of various methods proposed to model intraoperative organ deformation, there are still few literature reviews that systematically categorize and summarize these approaches. This review aims to fill this gap by providing a comprehensive and technical-oriented overview of modeling methods for intraoperative organ deformation in augmented reality in surgery. Through a systematic search and screening process, 112 closely relevant papers were included in this review. By presenting the current status of organ deformation modeling methods and their clinical applications, this review seeks to enhance the understanding of organ deformation modeling in AR-guided surgery, and discuss the potential topics for future advancements.

## KEYWORDS

Augmented reality, organ deformation modeling, non-rigid registration, surgical navigation

## 1. Introduction

Recent advancements in optical see-through displays have introduced augmented reality (AR) as a promising tool for surgical navigation [1]. In AR-guided surgery, 3D digital organ models can be overlaid onto real anatomical structures [2]. These organ models are generated from patient-specific data obtained through preoperative computed tomography (CT) or magnetic resonance imaging (MRI) images. They encompass information that presents organ shapes, surfaces, blood vessels, and tumors. The alignment of these digital models with patient anatomy helps surgeons to form an intuitive understanding of the spatial relationships among various anatomical structures concealed beneath the organ surfaces (see Figure 1). The improved spatial awareness alleviates the burden for surgeons in localizing the safety-critical structures. This facilitates the execution of surgical plans with a higher level of precision and more informed decisions that could contribute to improved surgical outcomes [3,4].

---

Corresponding author: Qi Dou (qidou@cuhk.edu.hk).

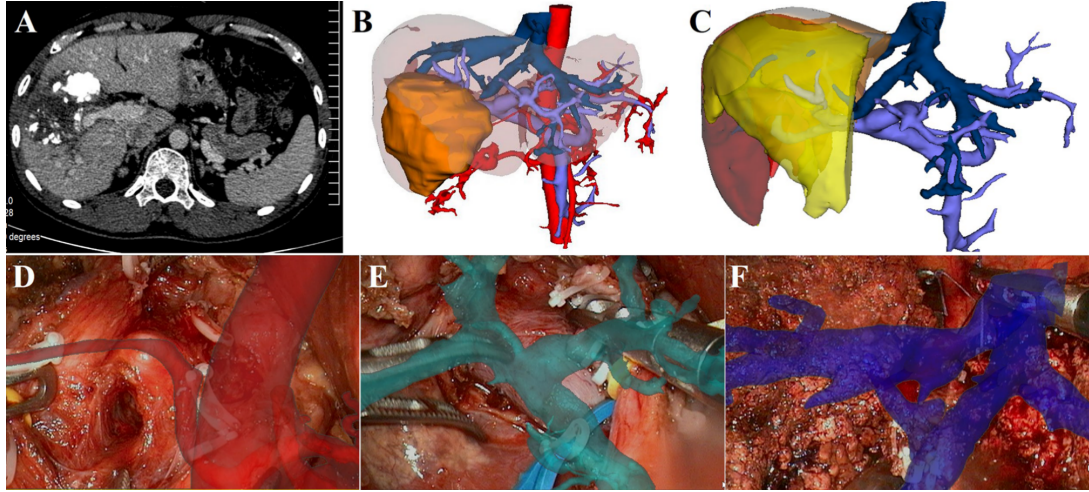


**Figure 1.** Surgical navigation using augmented reality with an illustrative example of hepatectomy [5]: A: preoperative CT images containing the liver; B: 3D reconstructed organ models for liver; C: residual liver volume from simulated right hepatectomy; D: intraoperative navigation of the hepatic artery; E: intraoperative navigation of the portal vein; F: intraoperative navigation of the hepatic vein. Permissions: images licensed from the reference [5] under CC BY 4.0.

Despite the potentials of AR-guided surgery, its reliability can be compromised by organ deformations caused by factors such as patient positioning, respiratory motion, extrinsic compression by pneumothorax, hematoma, or the device [6,7]. These deformations lead to misalignment between the preoperative digital organ models and the intraoperative anatomy, affecting the accuracy of localizing tumors and vessels [8]. To make reliable surgical navigation, organ deformation modeling technique is an indispensable component in the AR-guided surgery system. This modeling process involves continuously adjusting preoperative 3D organ models to adapt to the dynamic deformations occurring during surgical procedures [9]. Organ deformations can be observed through various modalities, including the locations of anatomical landmarks [8,10], tissue structure silhouettes [11], or 3D digitized organ surfaces [12,13]. Organ deformation modeling, at its core, involves extrapolating organ deformation fields based on these intraoperative observations to adjust preoperative digital organ models.

While organ deformation modeling plays a pivotal role in AR-guided surgery, achieving consistency between digital models and real organs remains a persistent challenge due to technical constraints. Firstly, organ surfaces often lack distinct features suitable for use as fiducials in deformation modeling, and the limited color and texture contrast in intraoperative imaging modalities further exacerbate this issue [14,15]. Secondly, the intraoperative observations available for deformation modeling are relatively limited, typically allowing only partial views of organs to be acquired [16]. Extrapolating deformations spread across the entire organ from such limited information poses a significant challenge, especially given the considerable deformation that soft tissues within organs may experience during surgical procedures [17]. Thirdly, different surgical specialties present unique challenges. For instance, organs such as livers and kidneys exhibit viscoelastic deformation behavior during surgery [18–20], while spinal structures deform due to their inherent flexibility [21]. In these regards, specialized deformation modeling methods should be tailored for each surgical specialty to effectively address the corresponding organ deformations.

To inspire potential solutions for addressing these challenges in the computer-

assisted surgery research field, this literature review commences by providing a comprehensive and technical-oriented summary of current deformation modeling techniques (cf. Sec. 3). Subsequently, it delves into various surgical specialties, offering detailed insights into the particular challenges faced by each specialty and presenting existing solutions (cf. Sec. 4). Finally, drawing on existing research, this review discusses future research possibilities (cf. Sec. 5).

## 2. Literature Search and Screening Process

The literature search and screening process were conducted according to the guideline of *Preferred reporting items for systematic review and meta-analysis (PRISMA)* [22]. Figure 2 shows the overview of our literature processing workflow.

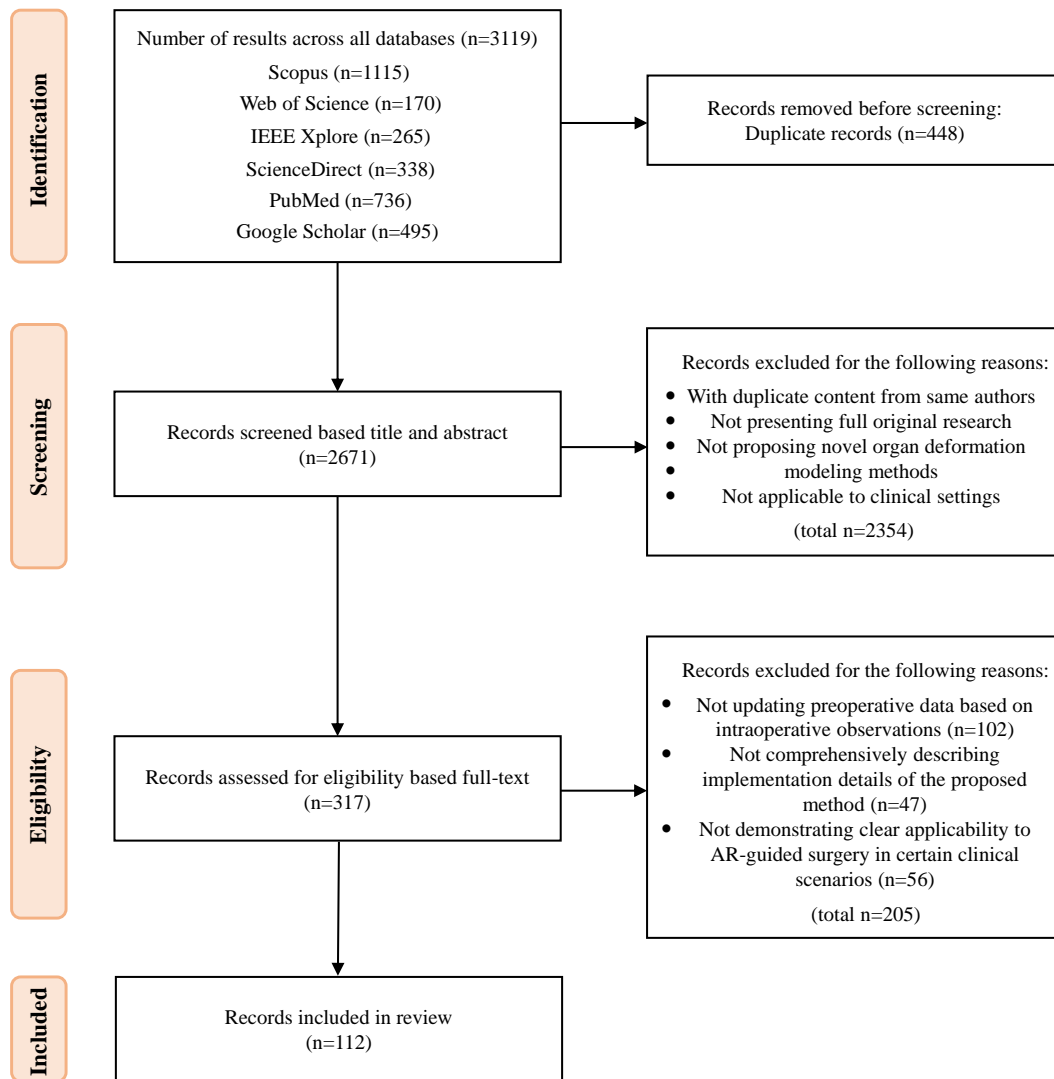


**Figure 2.** The workflow of the screening process using PRISMA [22] protocol for the performed review.

### ***2.1. Literature search***

The literature search was initially conducted in May 2023, across five scientific databases: Scopus, Web of Science, IEEE Xplore, ScienceDirect, and PubMed. An updated search on Google Scholar for 2023 and 2024 articles was subsequently performed on in March 2024 in order to add more literature including ArXiv papers. To make a comprehensive investigation, a number of search terms was identified, comprising keywords including “intraoperative”, “non-rigid”, “deformation”, “registration”, “modeling”, and “AR”. Logical operators (AND/OR) were utilized to combine the keywords, facilitating a thorough and proper retrieval of relevant articles from each database. A detailed list of these search terms can be found in Appendix Table A.1.

### ***2.2. Selection process***

The literature search yielded a total of 3119 records, and after removing duplicates, 2671 unique studies underwent screening. During the screening phase, titles and abstracts were reviewed to preliminarily exclude irrelevant publications. The exclusion criteria comprised the following items: (1) studies containing similar content from the same authors, (2) non-original research such as reviews or book chapters, (3) studies not focusing on modeling organ deformation, (4) studies not proposing new methods (e.g., comparative studies evaluating existing methods), and (5) studies not validated in scenarios related to clinical settings (e.g., focused solely on medical simulations or virtual surgical scenarios). Based on these criteria, 2354 records were excluded.

Subsequently, a more time-consuming full-text assessment was conducted to determine the eligibility of the remaining 317 studies for inclusion to this survey. Full-text articles had to satisfy the following inclusion criteria: (1) updating preoperative reconstructed 3D organ models based on information extracted from an intraoperative acquisition, (2) providing a comprehensive description of the proposed method’s implementation details, and (3) demonstrating clear applicability to AR-guided surgery in certain clinical scenarios. After applying these criteria, a final set of 112 studies were included in this review paper. In this way, we hope that the screened compact set of references can present the most closely-related literature and highly-informative summary, so that readers can find a focused survey on the specific topic of organ deformation modeling approaches in AI-guided surgery.

### ***2.3. Related review papers***

To ensure new knowledge provided by this review, we also examine existing survey papers on related topics identified during the literature search and screening process.

Min et al. [23] (2023) review registration approaches for aligning preoperative organ models with intraoperative anatomy. However, their focus is solely on orthopedic surgery and thus does not cover the deformation of soft tissues. Similarly, Gsaxner et al. [24] (2023) summarize methods for rigidly aligning digital and physical coordinates to realize surgical navigation in augmented reality space, but compensation for soft tissue deformation is still lacking. Schneider et al. [25] (2021) provide a comprehensive comparison of current surgical navigation systems with augmented reality support, regarding accuracy performance in laparoscopic liver surgery. While they discuss the issue of soft tissue deformation, a technical overview of how to model organ deformation is not provided. The most pertinent review on organ deformation modeling techniques is by Bernhardt et al. [1] (2017), who summarize non-rigid registration



methods to account for soft tissue deformation. However, this review was published a while ago, therefore a newer survey is needed to update the latest literature especially learning-based and data-driven techniques.

### 3. Organ Deformation Modeling Approaches

Organ deformation modeling involves predicting a deformation field as output to update a pre-surgery reconstructed 3D organ model based on the input intraoperative observations [9]. These observations can be anatomical point coordinates, or partial organ surface reconstructed from stereoscopic images, as illustrated in Figure 3. By incorporating these observations, the modeling process ensures the fidelity of preoperative organ models to intraoperative anatomical changes, thus accommodating tissue deformations during AR-guided surgery. With the potential to enhance the surgical precision, this field has attracted widespread attention, leading to the flourishing of various modeling algorithms.

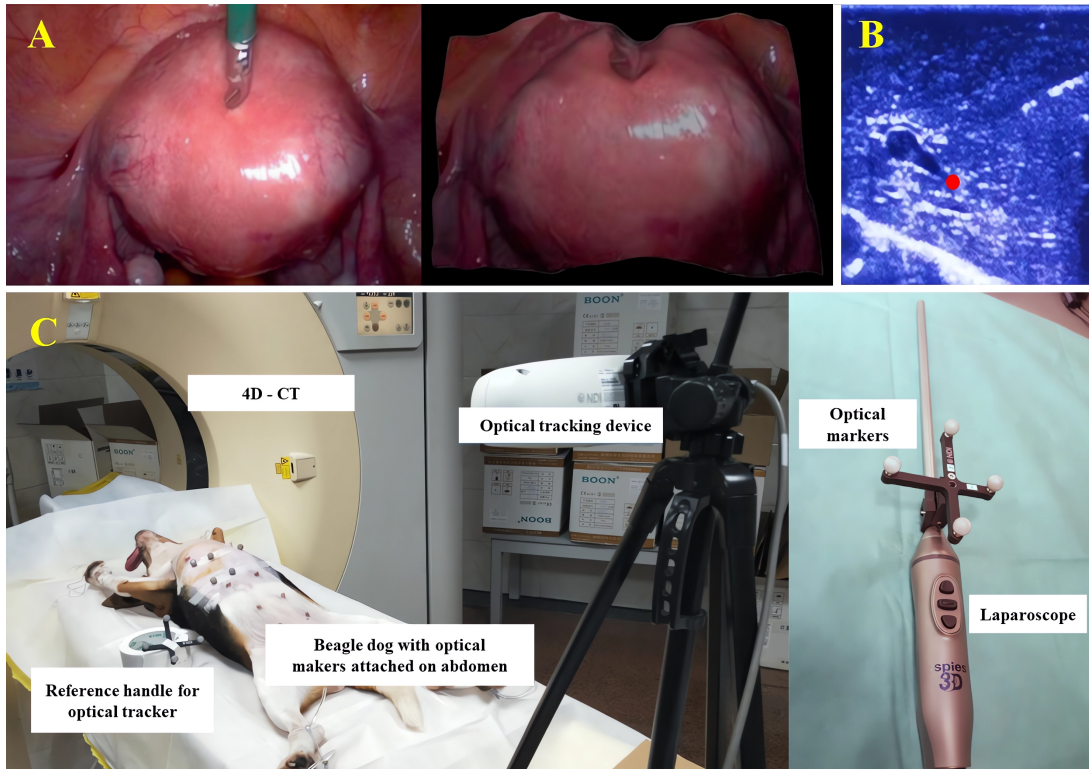


**Figure 3.** Illustration of several common intraoperative observations. A: reconstructed organ surface (right) from laparoscopic images (left); B: the position of anatomical points (red points) manually picked by surgeons on Ultrasound images; C: optical markers attach on the abdomen (left) and instruments (right). Permissions: some illustrative images reprinted from representative references [1,26,26] under respective copyright license permission from Elsevier.

#### 3.1. Categorization of organ deformation modeling methods

Existing algorithms for modeling organ deformations can be broadly categorized into model-based, data-driven, and hybrid methods. Table 1 and Table 2 provide a cate-

gorical summary of these existing methods for organ deformation modeling.

### 3.1.1. Model-based methods

In the field of organ deformation modeling, the majority of research efforts were initially directed towards model-based algorithms. These early research endeavors centered around understanding the tracking and modeling of tumor movement within organs during respiratory motion patterns. Clinical trials conducted by Schweikard et al. [27] confirmed the hypothesis that a correlation exists between internal and external motion. This discovery laid the foundation for the development of correlation models, which could predict the intraoperative motion of internal tumors based on changes in externally trackable signals, often referred to as surrogates. Correlation models found practical application in cases such as radiofrequency ablation therapy [13], where small tumors could be treated as rigid targets. However, when dealing with the deformation of soft tissues, correlation modeling proved to have limitations in its fitting capacity, presenting challenges [28].

To achieve the goal of modeling soft tissue deformations, further exploration ensued. Existing model-based algorithms can be categorized into four subcategories based on their underlying principles: (1) biomechanical models, (2) physics-based modeling methods, (3) geometry-based alignment methods, and (4) statistical models.

Biomechanical models ( $n = 44$ ) account for soft tissue deformations by numerically solving partial differential equations associated with constitutive models [29]. Finite element (FE) methods are commonly used in the numerical solving process due to their effectiveness in handling partial differential equations (PDEs). In biomechanical modeling, the problem of inferring organ deformation is framed as solving a boundary value problem, where the boundary conditions (input data) are derived from intraoperative observations [16]. Boundary conditions (BCs) on an FE model can be expressed as either displacements or forces. When specifying a displacement BC, a node is compelled to move to a given position. Conversely, when a force BC is specified, it ensures that the internal stress is in equilibrium with the applied stress. With specified BCs, biomechanical models have demonstrated promising capabilities in simulating the viscoelastic behavior of soft tissues within various organs, such as the liver, prostate, kidney, and brain [18–20,30]. However, their application in a real surgical setting encounters difficulties. Firstly, acquiring BCs during surgery remains challenging. Obtaining displacement BCs requires known surface correspondences, while obtaining force BCs necessitates precise measurement of forces applied by surgical tools on the organ [31]. Secondly, directly solving FE-based biomechanical models presents logistical limitations, such as the lengthy computational time [32]. These challenges limit the practical utility of biomechanical models in clinical scenarios. To address the issues, Yang et al. [33] recently proposed a boundary constraint-free biomechanical model, eliminating the need for predefined zero-displacements and force locations in BCs. Min et al. [34] explored the use of physics-informed neural networks to solve PDEs, offering potential solutions to computational efficiency challenges.

Physics-based modeling ( $n = 6$ ) presents an alternative approach to soft tissue deformation modeling. The fundamental concept behind these methods is to depict organ deformation in a physically interpretable manner. For instance, in the work by Suwelack et al. [35], the non-rigid deformation problem is likened to an electrostatic-elastic scenario, where an elastic representation of the preoperative liver model behaves akin to an electrically charged object interacting with the oppositely charged rigid intraoperative liver surface. The preoperative liver in its undeformed state and

the intraoperative liver surface, captured through stereo endoscopic imaging, serve as inputs for the registration process. Electrostatic forces facilitated the alignment of the preoperative liver with the intraoperative surface, with elastic forces providing regularization. Another approach, demonstrated by Dagon et al. [36], involved modeling hepatic vein deformations using a mass-spring skeleton aligned with vessel centerlines. During surgery, the actual vessel positions were inferred from image segmentation provided by a tracked 2D ultrasound system. These intraoperative measurements were then translated into 3D points, serving as input data. Elastic deformation of the skeleton to align with these 3D points was achieved by applying virtual forces until it conformed to the measurements. Currently, research in physics-based modeling remains relatively limited, and there is a need to explore additional physical constraints to enhance the realism of deformation modeling [37].

Geometry-based alignment methods ( $n = 21$ ) handle 3D organ models in the form of point clouds. These methods deform the preoperative 3D organ model by manipulating its geometric coordinates, specifically the 3D points that compose the organ surface [38]. They aim to find a rigid transformation while simultaneously deforming the preoperative 3D model (output) to align it with the intraoperative organ surface point clouds (input data). This is achieved by employing non-rigid point cloud registration algorithms, such as multi-stage iterative closest point (ICP), coherent point drift (CPD), or thin-plate spline (TPS) registration [12,39,40]. These algorithms estimate point correspondences and transformation functions between preoperative and intraoperative surfaces, aiming to maximize the alignment of visible regions between preoperative and intraoperative surfaces [41]. However, rather than FE-based or physics-based approaches, geometry-based alignment methods often lack strain energy regularization [42] in the deformation modeling process. This regularization, described by the material properties and geometric features of organs, ensures that the deformation results adhere to organs' elastic properties and mechanical behavior. The absence of this regularization in geometry-based alignment methods can diminish the accuracy and reliability of the predicted deformations in invisible surface regions. Moreover, geometry-based alignment methods face challenges in effectively propagating external organ surface deformation to internal structures such as vessels and tumors. In a preliminary study conducted by Maris and Fiorini [40], a direct application of the non-rigid TPS function obtained from the surface registration to each of the points  $x$  of the target tumor was tested, resulting in an evaluation error of around  $5mm$  on the centroid of the tumor volume.

Statistical models ( $n = 9$ ) describe the patterns of organ shape variations or motion from a statistical perspective, corresponding to statistical shape models and statistical motion models. In the shape model, variations among shapes from different individuals are accounted for, while the motion model captures the temporal changes in shape relative to a reference, such as those caused by respiratory motion [43]. Constructing statistical models depends on having patient ground truth data, ideally offering high-resolution 3D spatial representations of organs. Particularly in the case of building statistical motion models, it is also crucial to have a sufficiently high temporal frame rate, capturing several volumes per second. To address the challenge of balancing image quality and acquisition speed, a learning-based technique was introduced by von Siebenthal et al. [44] to obtain 4D-MRI data. With the 4D-MRI data, a population-based statistical model can be built from the non-rigid registration of the MRI images [45,46]. The constructed statistical models can be employed to estimate present shape changes based on intraoperative observations. For instance, if online ultrasound images depict parts of the changing shape of interest, the full changing shape can be estimated

form the previously observed shape changes, which have been encapsulated in the statistical motion model.

In general, model-based methods employ explicit mathematical models to characterize organ deformation. Among these, biomechanical models demonstrate good simulation effectiveness for deformations induced by external forces, such as instrument interactions and pneumoperitoneum pressure. For deformations arising from regular motion patterns, such as those caused by respiratory motion, statistical models are more suitable. Physics-based modeling endeavors to transfer existing physical models to directly simulate the viscoelastic behavior of soft tissues. Geometry-based alignment methods, on the other hand, tend to utilize non-rigid registration techniques from general computer vision to simultaneously address organ rigid registration and deformation modeling. However, this approach often lacks strain energy regularization, thereby failing to ensure that the predicted results adhere to organs' elastic properties and mechanical behavior.

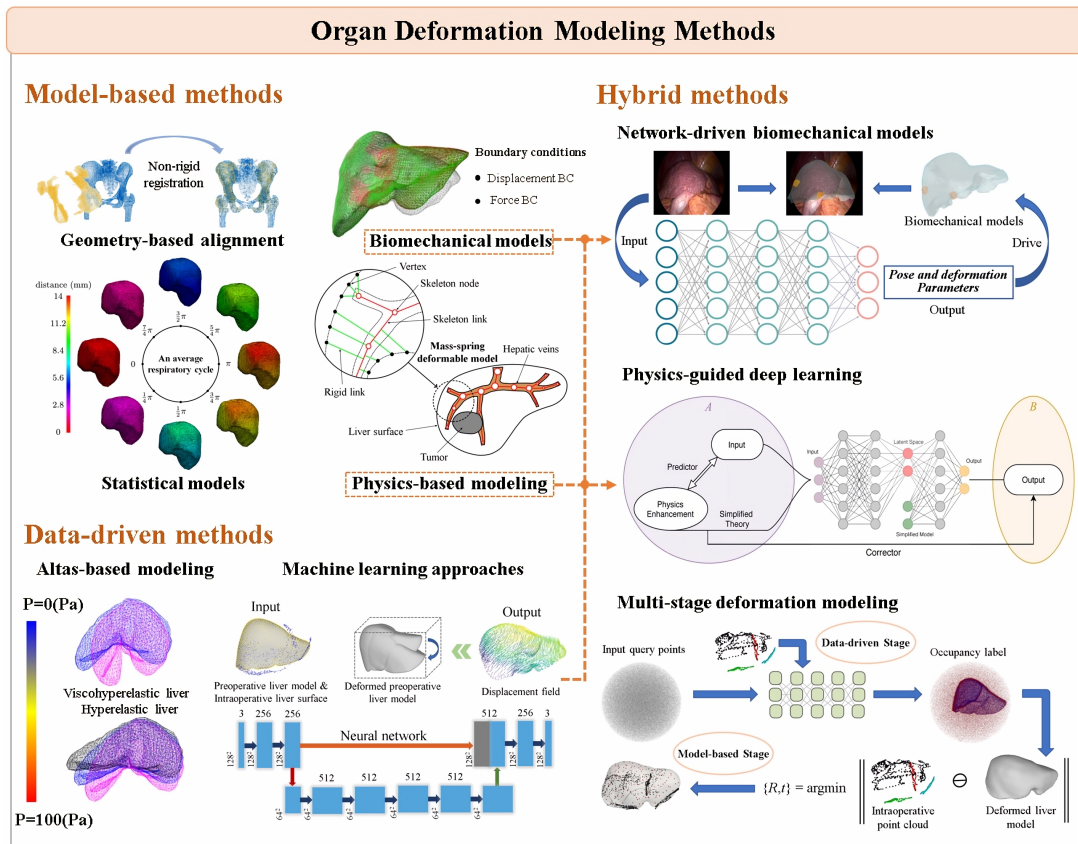


**Figure 4.** Overview of deformation modeling methods: (a) Model-based methods include: geometry-based alignment methods, biomechanical models, statistical models, and physics-based modeling. (b) Data-driven methods include: atlas-based modeling, and machine learning approaches. (c) Hybrid methods include: network-driven biomechanical models, physics-guided deep learning, and multi-stage deformation modeling methods. Permissions: some illustrative images reprinted from representative references [36,43,47–52] under respective copyright license permission from Elsevier, IEEE, CC BY 4.0, or AIP Publishing.

### 3.1.2. Data-driven methods

Data-driven methods were initially employed to address the limitations of directly applying biomechanical models in surgical procedures. Specifically, early data-driven methods sought to reduce intraoperative computation of biomechanical models by constructing a patient-specific atlas generated by FE-based simulation [32]. Recently, there has been a growing trend in adopting machine learning approaches as implicit representations of the underlying biomechanical model mechanism. The advantage of this adoption lies in the ability of machine learning approaches to predict the complex behavior of elastic organ structures in real-time without relying on preassigned boundary conditions [10]. This is particularly beneficial for clinical applicability, as boundary conditions are often challenging to obtain in clinical settings. The following provides an overview of the utilization of (1) atlas-based modeling approaches and (2) machine learning approaches in deformation modeling.

The atlas-based method ( $n = 5$ ) entails the construction of a pre-operatively computed collection of solutions, referred to as an atlas. This atlas is then used to align the data acquired during surgery with the solutions within the atlas, enabling the prediction and correction of the intraoperative organ deformation [53]. The process of atlas construction begins with the generation of a patient-specific finite element organ model. This model is derived from the surface description provided by a segmentation of the pre-operatively obtained image volumes. Boundary conditions, patient orientations (e.g., gravity directions), and material properties are selected based on a priori knowledge of surgical loading conditions [54]. The preoperative FE organ model is then run for each combination of conditions to create the atlas of organ deformation solutions. During surgery, a set of weight parameters (output) is determined to linearly combine the pre-operatively computed collection of solutions within the atlas [55]. This allows the organ model generated from atlas to match with the intraoperative observations, such as 3D digitized surfaces of the organ (input). These weight parameters can be iteratively solved using various algorithms, such as the iterative closest atlas algorithm [32] or the Levenberg–Marquardt nonlinear optimization method [56].

Machine learning approaches ( $n = 10$ ) were initially harnessed to expedite biomechanical modeling [57]. These models learn a function that maps inputs, such as external forces, to outputs, such as nodal displacements, by training on organ deformation datasets [58]. Typically, these datasets consist of synthetic data generated from simulating the biomechanical behavior of organs using FE methods [59]. Training the network using synthetic datasets rather than real patient data is a trade-off. Collecting ground truth deformation patterns of the same patient’s organs would require multiple CT scans, which is impractical in clinical practice. Notably, studies such as [29,31,60–62] have shown that even when trained solely on synthetic data, machine learning models still have the potential to accurately predict the physical deformation behaviors of organs. After training, the machine learning model serves as an implicit representation of the underlying biomechanical model mechanism, eliminating the need for explicit mathematical formulations during inference. Further, machine learning approaches can be categorized into two main branches: traditional machine learning (TML) and deep learning (DL) techniques. Specifically, traditional machine learning techniques, such as support vector machines and random forests, have demonstrated their potential to simulate tissue behavior in real-time, including organs such as breasts [63] and livers [64,65]. However, these methods face limitations when applied in actual surgical settings. Traditional machine learning models rely on FE-based conditions, specifically stress and displacement conditions [66], as input variables. Acquiring these variables

in a real surgical environment is challenging, since, for instance, measuring forces requires additional devices, and estimating surface displacements necessitates knowledge of surface correspondences [31]. Currently, the most widely adopted solution for obtaining input variables involves simplified boundary conditions, which assume fixed subsets of nodes while leaving others free [67–69]. However, manually assigning these boundary conditions can lead to instability if incorrect values are chosen, thereby impeding prediction accuracy. Deep learning, on the other hand, has been recognized as a powerful approach for predicting organ deformation behaviors, offering enhanced clinical applicability due to its ability to operate in real-time and independence from preassigned boundary conditions. These algorithms function by taking preoperative organ models, along with intraoperative observations such as 3D reconstructed organ surfaces (input), and predicting a displacement field (output) that warps the preoperative models to align with these intraoperative observations. For instance, Nakao et al. [70] introduced a deep learning-based framework for modeling the deformation of abdominal soft organs. This framework offers an end-to-end solution for real-time 2D/3D deformable registration by integrating an image-based generative network [71] and a graph convolutional network (GCN) [72]. The generative network learns the transformation from the 2D projection image to a displacement map, while the GCN translates this transformation into the final nodal displacements of the organ model. Moreover, Pfeiffer et al. [31] harnessed a fully 3D convolutional architecture to recover the displacement field directly from the intraoperative digitized organ surface, which was reconstructed from the laparoscopic video. This estimated displacement field can subsequently be utilized to deduce the nodal displacements spanning the entire organ, encompassing organ surface, vessels, and tumors. Table 4 summarizes publicly available datasets that can be used for neural network training and quantitatively evaluating accuracy.

In general, data-driven models, by learning a vast number of deformation patterns, can serve as implicit representations of the underlying biomechanical mechanism. Thanks to parallel computing, the inference process of data-driven methods can be significantly accelerated [48]. Additionally, both atlas-based methods and deep learning approaches can directly infer deformation fields from intraoperative observations, greatly enhancing clinical applicability [29,31,62]. In contrast, traditional machine learning methods still rely on manually assigning boundary conditions, which can lead to instability and affect accuracy if incorrect values are chosen.

### 3.1.3. Hybrid methods

Hybrid methods represent the fusion of model-based and data-driven approaches, offering notable flexibility in their implementation.

One approach to implementing hybrid methods involves leveraging network-driven biomechanical models ( $n = 4$ ). This approach utilizes neural networks to estimate essential prerequisites, such as boundary conditions or deformation parameters, to drive biomechanical organ models. These prerequisites are typically challenging to directly measure during actual surgical procedures. An example to better illustrate this concept is the work of Tagliabue et al. [73], who employed a BANet [74] to continuously estimate boundary conditions from raw intraoperative point cloud data of the deforming anatomy, captured by a vision sensor. The estimated boundary conditions from BANet guide preoperative biomechanical organ models to deform, ensuring an accurate representation of intraoperative organ deformations. Another example comes from the work of Labrunie et al. [49], where neural networks predict pose ( $R$ ,  $T$ ) and deformation

parameters ( $\beta$ ) defining the intraoperative state of the organ. Initially, a ResNet-50 network [75] extracts organ boundary features from mini-invasive images. These extracted features, along with the temporary pose ( $R, T$ ), and deformation parameters ( $\beta$ ), serve as inputs to a regression network [76]. This network iteratively updates the pose ( $R, T$ ) and deformation parameters ( $\beta$ ), which are subsequently employed to drive the preoperative biomechanical organ model for an accurate representation of organ deformations.

Another method for implementing hybrid approaches involves multi-stage deformation modeling ( $n = 10$ ), which breaks down the deformation modeling process into multiple stages and selecting appropriate methods for each. For example, Shi et al. [10] decomposed organ deformation modeling into organ surface and internal structure deformation modeling stages. Initially, an external-internal correlation model [77] is used to estimate organ surface deformation by tracking the displacement of external markers attached to the skin. Subsequently, neural networks propagate the surface deformation to internal structures, such as vessels and tumors. Meanwhile, Jia and Kyan [17] achieved deformation modeling by first recovering organ shape and then performing non-rigid registration. They utilized a point cloud occupancy network [78] to infer the complete organ shape from partial organ surfaces. Then, a correction algorithm utilizing the Levenberg–Marquardt nonlinear optimization method [79] is applied for non-rigid registration based on the organ shape inferred from the network.

Implementing hybrid methods through physics-guided deep learning ( $n = 3$ ) presents another viable solution. This approach incorporates established physical principles, equations, and laws into the training and inference process of deep learning models to ensure that the models’ predictions align with physical phenomena [80]. Pioneering work in this field was introduced by Min et al. [34], who employed a novel deep learning approach integrating physics-informed neural networks (PINNs) with PointNet for non-rigid medical image registration. The key physical principle integrated into the deep learning model is a loss function term based on biomechanical constraints, which ensures that the estimated spatial transformation is biophysically plausible. This method represents prostate point displacements using PointNet[81], while PINNs impose elastic constraints on the estimated displacements. Comparison experiments have illustrated that incorporating these physics-guided constraints significantly reduces target registration error, especially for patients with large deformations, thereby demonstrating superior performance and generalizability to new subjects.

In general, hybrid methods effectively leverage the strengths of both data-driven and model-based approaches. They can improve data-driven predictions to better approximate the viscoelastic characteristics observed in actual organs, or expedite model-based methods in acquiring the necessary prerequisites for controlling organ models. The flexibility in implementing hybrid methods can also expand their applicability in real clinical settings.

### ***3.2. Comparison of different deformation modeling methods***

We would like to compare different deformation modeling methods based on their accuracy, computational efficiency, and ease of implementation, categorizing their performance as “high”, “medium”, or “low” for each criterion. The “accuracy” criterion evaluates the method’s ability to accurately predict the deformation behavior of soft tissues; “computational efficiency” indicates its suitability for real-time applications;



and “ease of implementation” reflects the method’s practical applicability in clinical settings, considering factors such as the ease of model construction, and the accessibility of required intraoperative observations (input data) during clinical practice.

### *3.2.1. Accuracy comparative analysis*

In terms of accuracy, methods utilized biomechanical FE-models best explain the deformation behavior induced by external forces. This is primarily due to the fact that this method is grounded in continuum mechanics theory [61]. Additionally, this method can leverage prior knowledge about the mechanical load applied to organs to reduce the complexity of the problem space. This prior knowledge can be integrated into constraints within the adjoint optimization scheme [82], or decomposed into a set of localized point forces distributed over the active contact surfaces of the organ to control deformation responses [83]. Conversely, methods that solely rely on surface correspondence and lack mechanical constraints, such as geometry-based alignment methods in model-based approaches, and data-driven methods, often lack strain energy regularization within the objective function, leading to limited control over deformation field irregularities. Additionally, deep learning approaches in data-driven methods may exhibit voxelization artifacts, associated with data discretization procedures at convolutional layers [51]. However, incorporating physics-guided loss functions for optimizing the parameters of the deep learning model has the potential to enhance accuracy in unseen deformation scenarios [84]. For deformations arising from regular motion patterns, such as those caused by respiratory motion, statistical models perform better. This is because statistical models are directly constructed from patient ground truth data. These models estimate evolving shapes based on previously observed shape changes encapsulated within the statistical motion model.

### *3.2.2. Computational efficiency comparative analysis*

Implementing parallel processing is key to ensuring computational efficiency. However, achieving this in FE-based methods poses challenges due to the memory access arrangement required for concurrent updates of matrix entries describing the physical state [85]. To overcome this obstacle, machine learning approaches have been effectively leveraged, benefiting from the parallelization capabilities of modern GPUs, to accelerate FE models [84]. By training on datasets generated from FE simulations, the machine learning model serves as an implicit representation of the underlying biomechanical model mechanism, eliminating the need for explicit mathematical formulations during inference. Similarly, deep learning models take advantage of parallelizing well on modern GPUs to extract complex patterns efficiently. As for other model-based methods, including statistical models, geometry-based alignment methods, and physics-based modeling, the algorithms themselves are not inherently complex and can be parallelized for computation. However, geometry-based alignment methods typically require an iterative optimization framework, which needs serial implementation, consequently diminishing some of their computational efficiency.

### *3.2.3. Ease of implementation comparative analysis*

The ease of model construction and the clinical accessibility of input data will both impact the applicability of methods in real clinical settings. Ideally, algorithms that do not require additional equipment for acquiring input data will have higher clinical applicability. Atlas-based modeling and deep learning methods in data-driven ap-

proaches, as well as physics-based modeling and geometry-based alignment methods in model-based approaches, can directly utilize organ surface information reconstructed from stereo 3D laparoscopy to predict organ deformations. Statistical models can also predict deformation behavior directly from 3D reconstructed organ surfaces; however, the construction of statistical models requires acquiring patient ground truth data at different respiration stages [43], thereby increasing the difficulty of the model construction phase. Moreover, biomechanical models require stress or displacement boundary conditions as input, which can be challenging to obtain in clinical practice. Acquiring stress boundary conditions necessitates measuring forces applied by surgical tools on the organ [31]. Displacement boundary conditions can be obtained by measuring the displacement of interacting instruments [29], but this also requires additional equipment for spatial tracking of the instruments. Consequently, acquiring input data for biomechanical models is more demanding compared to other methods. Utilizing neural networks to estimate boundary conditions for driving biomechanical organ models holds promise for expanding their utility in clinical settings [73].

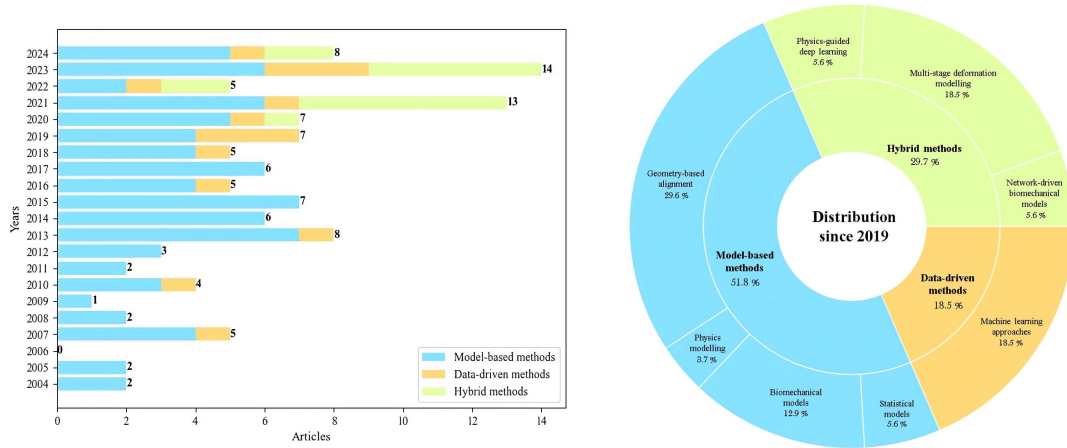


Figure 5. Annual distribution of articles focusing on organ deformation modeling methods.

### 3.3. Analysis of annual distribution of relevant methods

We further analyze the annual distribution of organ deformation modeling methods to understand their evolution over time. Figure 5 presents charts showing the annual distribution of articles focusing on these algorithms, revealing trends and patterns within the research landscape.

Between 2004 and 2018, research efforts primarily focused on model-based algorithms, underscoring their significance. Afterwards, starting in 2019, there was a noticeable increase in studies using neural networks to directly infer organ deformations from intraoperative observations, without manual parameter assignments. This shift led to the emergence of hybrid algorithms, combining both model-based and data-driven approaches. Notably, in 2020, there was a surge in articles on hybrid algorithms, reaching a comparable level with those on model-based algorithms. This rise reflects growing recognition of the benefits of integrating both approaches. Through a synergistic combination of model-based and data-driven methodologies, it is possible to refine data-driven results to better emulate the viscoelastic characteristics of real organs, or accelerate model-based methods in obtaining essential prerequisites for de-

forming organ models. As the field evolves, ongoing development of hybrid algorithms holds great promise for advancing the accuracy and efficacy of deformation modeling in clinical applications.

#### 4. Clinical Applications of Deformation Modeling for AR-guided Surgery

Organ deformation modeling has been explored across different surgical specialties to mitigate disparities between preoperative and intraoperative anatomical states, aiming to enhance the precision of surgical procedures. Figure 6 illustrates the distribution of research publications across these surgical specialties. Each specialty presents its own challenges, demanding tailored solutions and implementations for addressing them. The subsequent section will delve into the implementation of organ deformation modeling methods in each surgical specialty, including hepatobiliary surgery, brain surgery, breast surgery, spine surgery, vascular surgery, and renal surgery.

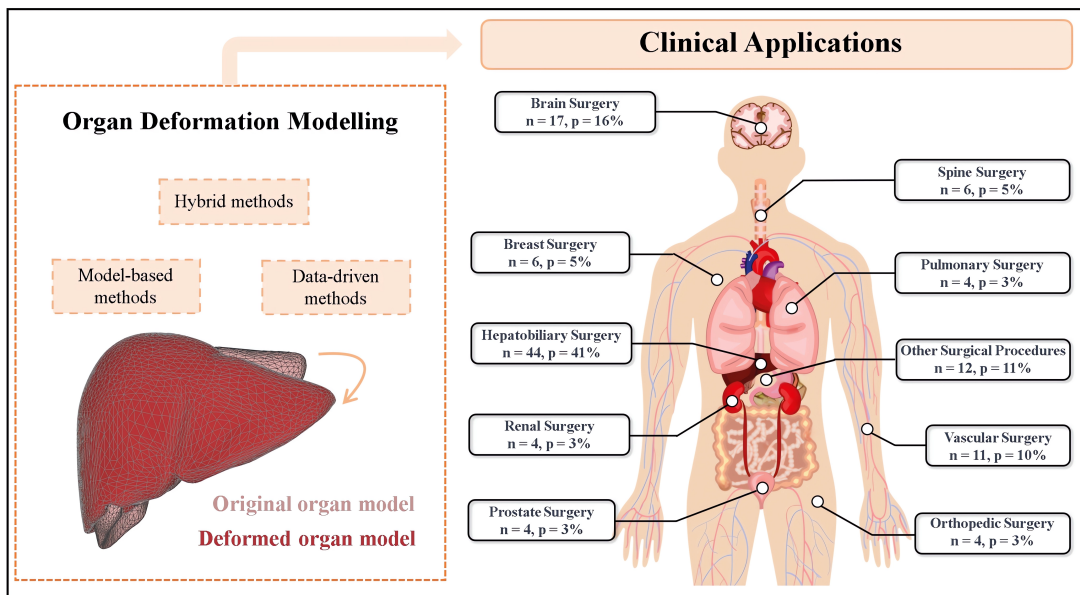


**Figure 6.** Overview of reviewed 112 articles grouped by surgical specialty in clinical application scenarios.

##### 4.1. Hepatobiliary surgery

Organ deformation modeling finds applicability in hepatobiliary surgery procedures, including percutaneous tumor ablation and liver resection.

In the context of percutaneous tumor ablation, the internal tumor position can be predicted in real-time from the external signals, such as the motion of trackable markers attached to the skin [86]. This is achieved by establishing the correlation between the internal tumor position and external signals via regression or statistical tumor motion models [87]. Furthermore, recent advancements [10,88] have shown that even the deformation of healthy tissue near tumors, such as blood vessels, can also be predicted from external signals using neural networks. This empowers surgeons to effectively plan optimal puncture trajectories and perform tumor destruction while minimizing damage to adjacent healthy tissues. To date, in animal experiments applying liver

deformation modeling, the exemplar achieved puncture accuracy is  $3.52mm$  (pig) [89] and  $2.50mm$  (dog) [10] in terms of targeting tumors, meeting the precision surgical safety requirement of an error less than  $5mm$  [90].

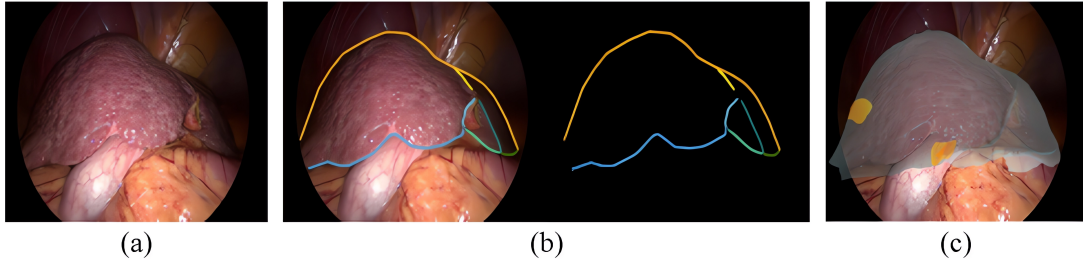


**Figure 7.** Example of Liver deformation modeling pipeline [49]. (a) Laparoscopic liver images; (b) extracted liver silhouettes; (c) projected deformed liver models. Permissions: images licensed under CC BY 4.0.

In the context of liver resection, challenges arise when dealing with soft-tissue deformation modeling. Firstly, the traction exerted by surgical instruments induces large viscoelastic deformation in the liver organ, particularly in laparoscopic surgery, where pneumoperitoneum introduction further amplifies liver deformation [3]. This deformation can greatly alter the spatial relationships among the liver’s internal tissues [6]. Secondly, in liver resection procedures, available intraoperative information for liver deformation modeling is relatively limited. Typically, only a partial surface of the liver can be observed, often through laparoscopic cameras or specialized depth sensors designed for liver surface digitization [91]. Inferring the deformation of the entire liver from this partial surface, especially given the lack of detailed texture information, presents a significant challenge [14,62]. To address these issues, Pfeiffer et al. [31] attempted to predict the displacement field of the entire liver directly from the deformed partial liver surface, reconstructed from intraoperative laparoscopic video streams. The predicted displacement field can then drive the deformation of the entire preoperative liver model, including the liver surface, vessels, and tumors. Results from *in silico* experiments indicate a strong correlation between the accuracy of liver deformation modeling and the degree of liver deformation as well as the visibility ratio of the liver surface. Labrunie et al. [49] pursued a similar approach to predict the liver’s displacement field from laparoscopic video. However, instead of reconstructing the liver surface, they employed a ResNet-50 encoder [75] to extract the liver’s 2D silhouettes, thereby imposing further constraints on liver deformation modeling (as shown in Figure 7). Accuracy experiments conducted in retrospective patient cases revealed a liver surface registration error of  $8.5mm$  in low deformation cases and  $16.4mm$  in cases involving large deformation.

#### 4.2. Brain surgery

The primary approach for treating brain tumors is surgical resection, with the extent of resection being highly correlated to patient survival rates [92]. However, the phenomenon of brain shift, characterized by non-rigid tissue displacement attributed to factors such as cerebrospinal fluid drainage, tissue swelling, and gravitational effects, introduces misalignment between preoperative imaging and real-time intraoperative conditions. The misalignment may considerably affect the surgical outcome since neurosurgical procedures are often based on pre-operative planning where brain shift is not considered [93,94].

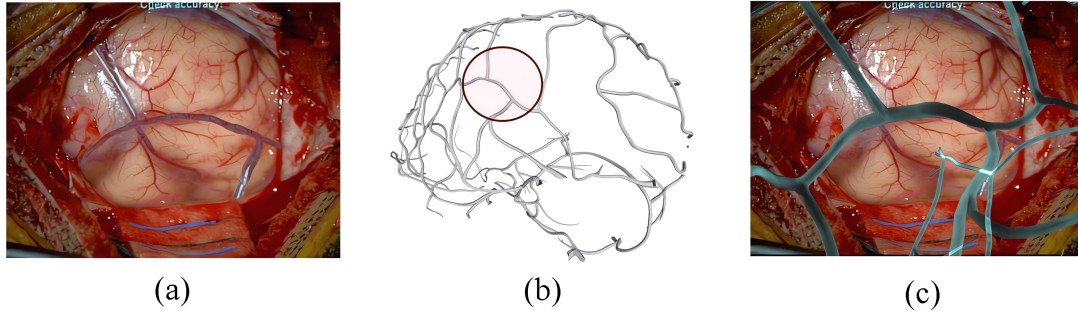


**Figure 8.** Example of AR-guided brain surgery with cortical brain vessels [95]. (a) intraoperative vessel image; (b) preoperative vessel model with region of interest; (c) pre- to intra-operative overlay with brain shift compensation. Permissions: images reprinted with permission from SPIE.

Modeling brain deformation is essential to maintain alignment between preoperative surgical planning and intraoperative conditions. In craniotomy, this demands a high level of accuracy since any errors could potentially affect critical brain functional areas [96]. Notably, the contours of cortical vessels, exposed on the brain parenchyma surface, offer distinct features that are instrumental in achieving high-precise deformation modeling (as shown in Figure 8). These vessel contours can be obtained through manual selection of points representing the starting and ending points of vessel segments [95] or by directly employing neural networks to extract them from microscopic images [97,98]. Extracted cortical vessel features can serve as valuable inputs for driving biomechanical model deformations [95] or as constraints for aligning preoperative models with intraoperative anatomy. In addition, some studies opt for an optimization approach to iteratively update the preoperative brain model, minimizing its displacement from the intraoperative 3D brain surface [53,54,94]. The intraoperative 3D brain surface is typically segmented from intraoperative magnetic resonance images [30] or directly acquired using a laser range scanner [99].

Currently, the assessment of deformation modeling accuracy is primarily carried out under in-silico conditions. Haouchine et al. [97] reported impressive accuracy, achieving a target registration error below  $1.93mm$  within the cortical level and immediate sub-cortical structures (depth  $\leq 15mm$ ) during in-silico evaluations. The brain shift compensation demonstrated effectiveness of up to 68.2%, with a minimum compensation of 24.6% even in the most challenging configurations [97]. However, errors exhibited an upward trend when targeting locations deeper within the brain (depth  $\geq 30mm$ ) or when confronted with greater degrees of deformation (depth  $\geq 6mm$ ) [97].

### 4.3. Breast surgery

Diagnosis of breast cancer relies on mammography and preoperative MRI, during which the patient is positioned either standing or lying prone with pendant breasts. However, when performing breast conserving surgery, the patient is typically in a supine or semi-vertical position for ultrasound (US) guided interventions [100]. These shifts in patient positioning invariably result in breast deformation between the diagnostic and biopsy phases under the influence of gravity. Additionally, the compression forces from the US probe can cause significant deformation and repositioning of breast anatomy [101]. The cumulative effect of these factors presents challenges to surgeons in accurately correlating tumor locations between medical images and the surgical field.



To model breast deformation arising from alterations in patient positioning, registration can be driven using sparse data compatible with acquisition during breast conserving surgery [100]. This sparse data includes corresponding surface fiducials, sparse chest wall contours, and the intra-fiducial skin surface. For instance, Ebrahimi et al. [102] observed deformations resulting from full abduction of the arm in supine MRI. They employed the thin plate splines registration algorithm, utilizing 24–34 fiducials evenly distributed across the breast surface, to rectify these deformations. Regarding deformation caused by the compression of the US probe, breast deformation can be predicted from the displacement of the US probe itself [29]. Since the US probe is treated as a rigid body, it is reasonable to assume that when the anatomy is deformed by the probe during image acquisition, points on the breast surface beneath the probe will be displaced to the same extent as the probe. The displacement of surface nodes in contact with the US probe can then be used to predict displacements across the entire breast [71]. This method of relying on surface displacement inferred from the spatial tracking of the US probe, instead of directly monitoring surface deformations (e.g., via an RGBD camera), acknowledges that probe-induced deformations are significant but localized. Additionally, the probe itself typically obstructs much of the deformed surface from the sensor’s view, rendering it challenging to directly measuring displacements of the contact surface [29]. A recent in-vivo experiment [100] involving seven different human subjects was conducted to assess the accuracy of breast deformation modeling. This evaluation, which focused on targeting an average of 22 subsurface markers, resulted in an average target registration error (TRE) of 6.3mm.

#### 4.4. Spine surgery

Spinal deformations occur during surgery due to the patient’s respiration and surgical interventions, resulting in a disparity between preoperative CT scans of the spine and intraoperative conditions. Conventional intraoperative image-guided modalities, such as X-ray imaging, pose risks of ionizing radiation exposure for both patients and surgeons due to the need for multiple scans [103]. Addressing intraoperative deformations and radiation exposure are common challenges encountered in spinal surgery [104].

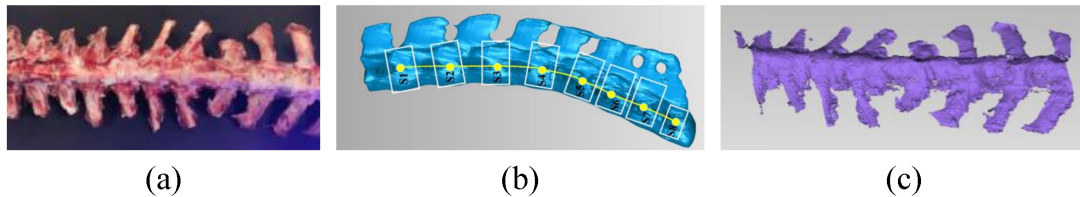


**Figure 9.** Example of spine surgery with spine animal models [39]. (a) The spine of a sheep; (b) preoperative 3D reconstruction and segmentation of spine based on CT; (c) intraoperative 3D reconstruction of spine based on binocular structured light. Permissions: images reprinted with permission from John Wiley and Sons.

Modeling spine deformation without relying on conventional intraoperative imaging modalities presents potential as a solution. The approach to implementing spine deformation modeling differs from that of other organ deformation modeling. To be specific, unlike viscoelastic organs such as the liver and brain, spine deformation arises from the inherent flexibility of spinal structures [21]. A spine can be segmented into several sections, and the deformation of the entire spine can be dissected into the deformation of each section (as illustrated in Figure 9). This concept is analogous to “breaking a curve into multiple straight lines”. For each segmented section, traditional rigid reg-

istration algorithms, such as bidirectional ICP [105], can be employed for modeling the deformation within each specific segment. As the registration progresses in each section, it culminates in local-to-global spine registration.

To reduce radiation exposure risks for both patients and medical staff, binocular structured light has the potential to acquire intraoperative spinal information instead of relying on traditional X-ray and CT scans. Chen et al. [39] utilized intraoperative spinal information obtained through binocular structured light to drive the aforementioned multi-section registration method, thereby facilitating spinal deformity correction while minimizing radiation exposure risks during surgery. Nevertheless, it is worth noting that their experiment was conducted in an in-vitro environment. Considering the difference in spine surface exposure extent between in-vitro and real surgical scenarios, further exploration of alternative imaging modalities remains imperative.

#### 4.5. Vascular surgery

Intraoperative interventions in vascular surgery encounter intricate vessel anatomy and demand real-time visualization. Currently, these interventions are primarily guided by intraoperative digital subtraction angiography (DSA) images [106]. However, the lack of critical 3D information within these images poses challenges for interventional radiologists in accurately identifying vessel branches, catheter tips, and the precise locations of narrowed coronary arteries [107]. Furthermore, the introduction of rigid endovascular devices exacerbates this challenge by inducing deformations that misalign intended treatments with actual interventions, potentially affecting treatment success and patient outcomes [108].

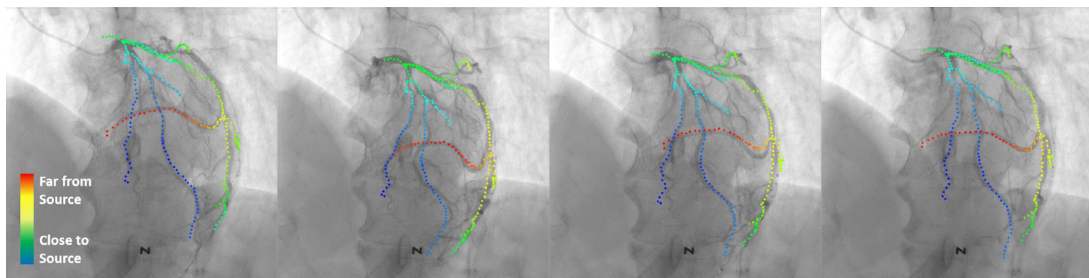


**Figure 10.** Example of vascular surgery with non-rigid registration of 3D vascular models and 2D DSA images [106]. From left to right is the registration of different frames. Permissions: images reprinted with permission from Elsevier.

To address the challenges mentioned above, deforming preoperative 3D vascular models and fusing them with intraoperative 2D DSA images show great promise [108]. This process can be achieved through 2D/3D non-rigid registration methods, where the goal is to iteratively minimize the center-line distance between the 3D vascular structures and the 2D vascular segments visible in DSA images. To tackle the cross-modal registration challenge between 3D vessel models and 2D DSA images, a graph-based representation of vessel tree geometry and topology [109] can be employed. Subsequently, graph matching algorithms, such as the adaptive compliance graph matching method [110] or the iterative closest graph matching method [107], can be applied to facilitate vascular registration. This approach finds applications in various vascular surgery scenarios, such as percutaneous coronary intervention for abdominal aortic aneurysms, or optimizing drug delivery and tumor targeting during intra-arterial therapies [111].



A recent 2D/3D non-rigid registration approach for vascular surgery was introduced by Yoon et al. [106]. They achieved a registration accuracy of  $1.98mm$  with respect to the distance error between 3D vessels and the 2D extracted vessels center-line, all while maintaining a computational efficiency of 0.54 seconds. This holds significant promise, as it suggests that surgeons can obtain precise visualizations and navigation within patient-specific vascular structures, ultimately leading to improved treatment strategies and enhanced patient outcomes.

#### ***4.6. Renal surgery***

Modeling organ deformation for surgical navigation is crucial in renal surgery, particularly in the context of minimally invasive procedures [112]. However, research dedicated specifically to organ deformation modeling in renal surgery remains relatively limited. To some extent, the methods for modeling renal deformation can draw insights from those employed in liver deformation modeling. This is because the challenges in modeling deformation in renal surgery and hepatobiliary surgery exhibit similarities. For instance, both renal and hepatic surfaces lack distinct texture features, and both organs undergo viscoelastic deformations [113].

A study by Zhang et al. [114] introduced a coarse-to-fine registration framework aimed at applying the coherent point drift algorithm to rectify kidney deformations in laparoscopic partial nephrectomy navigation. Subsequent optimization in their study [12] improved the accuracy and robustness of this framework against substantial deformations, supported by quantitative evaluations. The average root-mean-square error of volume deformation measured at  $0.84mm$ , and the mean navigation TRE from phantom experiments stood at  $1.69mm$ .

#### ***4.7. Summary of deformation modeling in surgical specialties***

In summary, the application of deformation modeling methods across various surgical specialties presents a diverse landscape with varying levels of research activity and implementation.

Hepatobiliary surgery takes a prominent position, with a large number of studies ( $n = 44$ ,  $p = 41\%$ ) focusing on liver resection and tumor ablation scenarios. While the radiofrequency ablation has achieved noteworthy precision (TRE less than  $5mm$ ) in animal experiments [10,13,89], studies concerning liver resection are still in the in-silico validation stage. Further exploration is needed to establish standardized clinical evaluation protocols and develop modeling algorithms capable of accurately predicting the complex behavior of soft tissues when subjected to large deformation [62].

In brain surgery ( $n = 17$ ,  $p = 16\%$ ), the contours of cortical vessels, exposed on the brain parenchyma surface, offer distinct features that are instrumental in achieving high-precise deformation modeling. Deformation modeling has demonstrated notable accuracy in mitigating disparities resulting from brain shift in-silico settings. Approaches involving non-rigid registration and the incorporation of biomechanical constraints have shown promising levels of accuracy, particularly in cortical and sub-cortical structures, achieving an impressive TRE below  $1.93mm$  [97]. Future endeavors should focus on further improving the accuracy of deeper brain regions and addressing real clinical situations characterized by pronounced degrees of deformation.

Breast surgery ( $n = 6$ ,  $p = 5\%$ ), spine surgery ( $n = 6$ ,  $p = 5\%$ ), vascular surgery ( $n = 11$ ,  $p = 10\%$ ), and renal surgery ( $n = 4$ ,  $p = 3\%$ ) have also witnessed the application

of deformation modeling methods, albeit with relatively more limited research activity and clinical implementation. In breast surgery, the deformation of breast can be predicted by the displacement of the US probe itself during compression. Data-driven models have shown promise in addressing challenges associated with mammography and ultrasound-guided procedures, showcasing an average TRE of  $6.3mm$  in clinical validation [100]. In spine surgery, a spine can be segmented into ‘n’ sections, and the deformation of the entire spine can be dissected into the deformation of each section. Multi-stage ICP approaches effectively harness the inherent structural characteristics of the spine to model intraoperative spine deformations, reducing reliance on traditional imaging methods for surgical navigation and thereby decreasing patient radiation exposure [39]. Vascular surgery utilizes deformation modeling to enhance spatial visualization and navigation within patient-specific vascular structures, leading to improved interventional procedures. This is achieved through the 2D/3D non-rigid registration of preoperative 3D models and intraoperative 2D images, resulting in an average distance error of  $1.98mm$  [106]. In renal surgery, Zhang et al. [12] have introduced registration frameworks to rectify kidney deformations during laparoscopic procedures, showcasing encouraging prospects for clinical applications, supported by a mean navigation TRE of  $1.69mm$  as evidenced from phantom experiments.

Beyond these, pulmonary surgery ( $n = 4, p = 3\%$ ), orthopedic surgery ( $n = 4, p = 3\%$ ), and prostate surgery ( $n = 4, p = 3\%$ ) emerge with limited studies delving into the application of deformation modeling. While holding promise, these fields are still in an evolutionary phase, warranting further exploration to delineate the most fitting utilization of deformation modeling techniques across their diverse scenarios.

Table 5 and Table 6 provide a summary of deformation modeling studies that have reported quantitative accuracy results. The metrics used to measure the performance of organ deformation modeling algorithms typically include TRE, Hausdorff distance (HD), and root mean square (RMS) error. However, it is essential to recognize that the assessment of accuracy is subject to various influencing factors. For instance, Pfeiffer et al. [62] have highlighted a direct correlation between algorithm accuracy and the extent of organ deformation. Substantial deformations, such as tissue pulling, often lead to larger absolute errors in algorithm predictions. Conversely, scenarios with minimal organ deformation, such as needle puncture, tend to yield more accurate predictions. Furthermore, the specific organs being studied and the utilization of different intraoperative observations can also directly impact algorithm accuracy. Therefore, it is prudent to consider the reported accuracy measurements as references for algorithm performance rather than the sole criteria for assessment.

## 5. Discussion on Current Status and Future Works

Organ deformation modeling serves as a dependable foundation for maintaining the consistency of preoperative organ models with the complex and dynamic intraoperative environment during AR-guided surgery. Overall, the current research field is still at a relatively preliminary stage, with remaining technical challenges to be tackled before possibility of wide adoption in clinical applications.

Existing algorithms for modeling organ deformations can be broadly classified into model-based, data-driven, and hybrid methods. Among these, biomechanical FE-models in model-based methods best explain the organ deformation behavior, and have been successfully applied to simulate the viscoelastic behavior of soft tissues. However, implementing these models directly in real surgical settings presents challenges due to

the prolonged computational time required. Specifically, numerical methods for solving the partial differential equations associated with biomechanical FE-models result in solving a system of linear equations. These linear systems are large, sparse, and often ill-conditioned, making traditional numerical solvers inefficient. To address this, leveraging learning-based approaches to obtain high-performing preconditioners offers a promising solution. The preconditioner should transform the original system into an equivalent one with more favorable properties for numerical solving, thereby making the system easier and faster to solve.

We consider exploring the integration of human guidance into the deformation modeling process shows promise for the next step. Currently, deformation modeling methods typically rely on pre-established surface correspondences. These methods estimate the movement of visible surfaces (those with established correspondences) with biomechanical constraints to propagate local motions for inferring the movement of non-visible surfaces. Therefore, establishing accurate correspondences is crucial for precise organ deformation estimation. However, organ surfaces often exhibit highly similar geometric features, such as the left and right lobes of the liver, leading algorithms to converge to incorrect correspondences and affecting the accuracy of subsequent deformation modeling. Existing algorithms struggle to handle such mismatches, especially for textureless surfaces. Incorporating human prior knowledge with carefully designed interaction and user interface in AR has the potential to address this challenge. The key to implementing this approach lies in finding the suitable interactive methods and efficiently leveraging the local reliable correspondence information in practice. Moreover, exploring methods to extend single-frame human annotations into sequential multi-frame data is an intriguing topic. Once humans provide reliable local surface correspondences for a specific deformation state, it is important to continuously utilize such information for subsequent deformations to reduce geometric feature ambiguity.

Furthermore, we also think that improving the accuracy performance of data-driven algorithms with limited data is a topic that warrants collective discussion in this field. The limited availability of data stems from the necessity of performing CT scans on patients during surgery to obtain ground-truth deformation of patient organs, thereby increasing the risk of radiation exposure for patients [31]. Although there are currently publicly available datasets (cf. Table 4) providing 3D organ models of patients in both preoperative undeformed and intraoperative deformed states, the dataset size is limited. Existing works mainly utilize the valuable data for quantitative evaluation in experiments rather than for training neural networks. There is a strong desire in this field to collect and release more data for research use. Synthetic data with ground truth deformation field are equally appreciated and popular at current status. Data efficient machine learning methods, such as transfer learning, self-supervised learning, foundation models, test-time adaptation have potentials for alleviating the problem.

Last but not least, ensuring patient safety through rigorous validation and testing protocols is essential. Currently, the accuracy of organ deformation modeling is primarily validated using phantoms or animal studies. Risk factors would be increasingly considered and more frequently discussed along with the advancement of pre-clinical validation of the AR navigation systems. Moreover, bias is a commonly reported issue in data-driven methods, potentially leading to unfair treatment and predicted outcomes. In organ deformation modeling, bias may arise from differences in patient’s organ morphology, severity of diseases, surgeon’s subjectiveness and incomplete understanding of deformation patterns. The reason behind this is also associated with the afore-mentioned issue of data scarcity. Finally, in relation to the ethical standards of intelligent navigation systems, if that are to be applied, building trust in

medical technology is crucial for its adoption. Breaking down the organ deformation prediction process into explainable, intuitive and sequential steps, rather than using a single end-to-end black box, can boost confidence in its clinical applications. This approach could allow surgeons to take over at any unsatisfactory step, leading to more reliable computer-assisted intervention as a whole. Addressing these intertwined issues requires multidisciplinary collaboration and sustained efforts to ensure safety, fairness, and ethical compliance in new technologies for healthcare.

## 6. Conclusion

This literature review presents a systematic and focused overview of methods for modeling organ deformation within the context of AR-guided surgery. We adopt a technology-driven narrative to trace the development and evolution of these modeling techniques. Furthermore, we extend our exploration to encompass various surgical specialties, shedding light on the current state of clinical applications for organ deformation modeling methods while identifying potential barriers to widespread clinical adoption. Building upon existing research, our aim is to provide insights into the future works of organ deformation modeling technology, with an emphasis on unresolved issues that require attention to enhance its applicability. Through this review, we hope to provide readers with an up-to-date understanding of the organ deformation modeling techniques which is fundamental for AR-guided surgery, while also raising interest of future investigations and contributions on this topic.

## Funding

This project was supported in part by the Science, Technology and Innovation Commission of Shenzhen Municipality (Project No. SGDX20220530111201008), in part by National Natural Science Foundation of China (Project No. 62322318) and in part by the Research Grants Council of Hong Kong Special Administrative Region, China (Projects No. N\_CUHK410/23 and No. T45-401/22-N).

## Disclosure of interest

No potential conflict of interest need to be reported by the authors in this publication.

## References

- [1] Sylvain Bernhardt, Stéphane A Nicolau, Luc Soler, and Christophe Doignon. The status of augmented reality in laparoscopic surgery as of 2016. *Medical Image Analysis*, 37: 66–90, 2017.
- [2] Manuel Birlo, PJ Eddie Edwards, Matthew Clarkson, and Danail Stoyanov. Utility of optical see-through head mounted displays in augmented reality-assisted surgery: A systematic review. *Medical Image Analysis*, 77:102361, 2022.
- [3] Huoling Luo, Dalong Yin, Shugeng Zhang, Deqiang Xiao, Baochun He, Fanzheng Meng, Yanfang Zhang, Wei Cai, Shenghao He, Wenyu Zhang, et al. Augmented reality navigation for liver resection with a stereoscopic laparoscope. *Computer Methods and Programs in Biomedicine*, 187:105099, 2020.

- [4] Jason YK Chan, F Christopher Holsinger, Stanley Liu, Jonathan M Sorger, Mahdi Azizian, and Raymond KY Tsang. Augmented reality for image guidance in transoral robotic surgery. *Journal of Robotic Surgery*, 14:579–583, 2020.
- [5] Weiqi Zhang, Wen Zhu, Jian Yang, Nan Xiang, Ning Zeng, Haoyu Hu, Fucang Jia, and Chihua Fang. Augmented reality navigation for stereoscopic laparoscopic anatomical hepatectomy of primary liver cancer: Preliminary experience. *Frontiers in Oncology*, 11: 663236, 2021.
- [6] Sylvain Bernhardt, Stéphane A Nicolau, Vincent Agnus, Luc Soler, Christophe Doignon, and Jacques Marescaux. Automatic localization of endoscope in intraoperative ct image: A simple approach to augmented reality guidance in laparoscopic surgery. *Medical Image Analysis*, 30:130–143, 2016.
- [7] Nadine Abi-Jaoudeh, Hicham Kobeiter, Sheng Xu, and Bradford J Wood. Image fusion during vascular and nonvascular image-guided procedures. *Techniques in Vascular and Interventional Radiology*, 16(3):168–176, 2013.
- [8] Fang Chen, Xiwen Cui, Jia Liu, Boxuan Han, Xinran Zhang, Daoqiang Zhang, and Hongen Liao. Tissue structure updating for in situ augmented reality navigation using calibrated ultrasound and two-level surface warping. *IEEE Transactions on Biomedical Engineering*, 67(11):3211–3222, 2020.
- [9] Naomichi Furushiro, Tomoharu Saito, Yoshitaka Masutani, and Ichiro Sakuma. Specification method of surface measurement for surgical navigation: Ridgeline based organ registration. In *International Conference on Medical Image Computing and Computer-Assisted Intervention*, pages 109–115. Springer, 2002.
- [10] Yangyang Shi, Xuesong Deng, Yuqi Tong, Ruotong Li, Yanfang Zhang, Lijie Ren, and Weixin Si. Synergistic digital twin and holographic augmented-reality-guided percutaneous puncture of respiratory liver tumor. *IEEE Transactions on Human-Machine Systems*, 52(6):1364–1374, 2022.
- [11] Igor Peterlík, Hadrien Courtecuisse, Robert Rohling, Purang Abolmaesumi, Christopher Nguan, Stéphane Cotin, and Septimiu Salcudean. Fast elastic registration of soft tissues under large deformations. *Medical Image Analysis*, 45:24–40, 2018.
- [12] Xiaohui Zhang, Tianmiao Wang, Xuebin Zhang, Yinghao Zhang, and Junchen Wang. Assessment and application of the coherent point drift algorithm to augmented reality surgical navigation for laparoscopic partial nephrectomy. *International Journal of Computer Assisted Radiology and Surgery*, 15(6):989–999, 2020.
- [13] Ruotong Li, Tianpei Yang, Weixin Si, Xiangyun Liao, Qiong Wang, Reinhard Klein, and Pheng-Ann Heng. Augmented reality guided respiratory liver tumors punctures: A preliminary feasibility study. In *SIGGRAPH Asia 2019 Technical Briefs*, pages 114–117. Association for Computing Machinery, 2019.
- [14] Ray A Lathrop, Tiffany T Cheng, and Robert J Webster III. Conoscopic holography for image registration: A feasibility study. In *Medical Imaging 2009: Visualization, Image-Guided Procedures, and Modeling*, volume 7261, pages 536–546. SPIE, 2009.
- [15] Thiago Ramos dos Santos, Alexander Seitel, Thomas Kilgus, Stefan Suwelack, Anna-Laura Wekerle, Hannes Kenngott, Stefanie Speidel, Heinz-Peter Schlemmer, Hans-Peter Meinzer, Tobias Heimann, et al. Pose-independent surface matching for intra-operative soft-tissue marker-less registration. *Medical Image Analysis*, 18(7):1101–1114, 2014.
- [16] Daniel Reichard, Dominik Häntsch, Sebastian Bodenstedt, Stefan Suwelack, Martin Wagner, Hannes Kenngott, Beat Müller-Stich, Lena Maier-Hein, Rüdiger Dillmann, and Stefanie Speidel. Projective biomechanical depth matching for soft tissue registration in laparoscopic surgery. *International Journal of Computer Assisted Radiology and Surgery*, 12:1101–1110, 2017.
- [17] Meng Jia and Matthew Kyan. Improving intraoperative liver registration in image-guided surgery with learning-based reconstruction. In *International Conference on Acoustics, Speech and Signal Processing*, pages 1230–1234. IEEE, 2021.
- [18] Alessandro Nava, Edoardo Mazza, M Furrer, Peter Villiger, and WH Reinhart. In vivo mechanical characterization of human liver. *Medical Image Analysis*, 12(2):203–216,

- 2008.
- [19] Mohamed Bader Boubaker, Mohamed Haboussi, Jean-François Ganghoffer, and Pierre Aletti. Finite element simulation of interactions between pelvic organs: Predictive model of the prostate motion in the context of radiotherapy. *Journal of Biomechanics*, 42(12): 1862–1868, 2009.
  - [20] Yannick Tillier, Audrey Paccini, Marc Durand-Reville, and J-L Chenot. Finite element modeling for soft tissue surgery based on linear and nonlinear elasticity behavior. *Computer Aided Surgery*, 11(2):63–68, 2006.
  - [21] Samuel Kadoury, Hubert Labelle, and Nikos Paragios. Automatic inference of articulated spine models in ct images using high-order markov random fields. *Medical Image Analysis*, 15(4):426–437, 2011.
  - [22] Matthew J Page, Joanne E McKenzie, Patrick M Bossuyt, Isabelle Boutron, Tammy C Hoffmann, Cynthia D Mulrow, Larissa Shamseer, Jennifer M Tetzlaff, Elie A Akl, Sue E Brennan, et al. The prisma 2020 statement: An updated guideline for reporting systematic reviews. *International Journal of Surgery*, 88:105906, 2021.
  - [23] Zhe Min, Ang Zhang, Zhengyan Zhang, Jiaole Wang, Shuang Song, Hongliang Ren, and Max Q-H Meng. 3d rigid point set registration for computer-assisted orthopedic surgery (caos): A review from the algorithmic perspective. *IEEE Transactions on Medical Robotics and Bionics*, 2023.
  - [24] Christina Gsaxner, Jianning Li, Antonio Pepe, Yuan Jin, Jens Kleesiek, Dieter Schmalstieg, and Jan Egger. The hololens in medicine: A systematic review and taxonomy. *Medical Image Analysis*, page 102757, 2023.
  - [25] Crispin Schneider, Moustafa Allam, Danail Stoyanov, DJ Hawkes, K Gurusamy, and BR Davidson. Performance of image guided navigation in laparoscopic liver surgery—a systematic review. *Surgical Oncology*, 38:101637, 2021.
  - [26] Lena Maier-Hein, Peter Mountney, Adrien Bartoli, Haytham Elhawary, D Elson, Anja Groch, Andreas Kolb, Marcos Rodrigues, J Sorger, Stefanie Speidel, et al. Optical techniques for 3d surface reconstruction in computer-assisted laparoscopic surgery. *Medical Image Analysis*, 17(8):974–996, 2013.
  - [27] Achim Schweikard, Greg Glosser, Mohan Bodduluri, Martin J Murphy, and John R Adler. Robotic motion compensation for respiratory movement during radiosurgery. *Computer Aided Surgery*, 5(4):263–277, 2000.
  - [28] Jamie R McClelland, David J Hawkes, Tobias Schaeffter, and Andrew P King. Respiratory motion models: A review. *Medical Image Analysis*, 17(1):19–42, 2013.
  - [29] Andrea Mendizabal, Eleonora Tagliabue, Jean-Nicolas Brunet, Diego Dall’Alba, Paolo Fiorini, and Stéphane Cotin. Physics-based deep neural network for real-time lesion tracking in ultrasound-guided breast biopsy. In *Computational Biomechanics for Medicine: Solid and Fluid Mechanics for the Benefit of Patients 22*, pages 33–45. Springer, 2020.
  - [30] Corey A Kemper, Ion-Florin Talos, Alexandra Golby, Peter M Black, Ron Kikinis, W Eric L Grimson, and Simon K Warfield. An anisotropic material model for image guided neurosurgery. In *International Conference on Medical Image Computing and Computer-Assisted Intervention*, pages 267–275. Springer, 2004.
  - [31] Micha Pfeiffer, Carina Riediger, Stefan Leger, Jens-Peter Kühn, Danilo Seppelt, Ralf-Thorsten Hoffmann, Jürgen Weitz, and Stefanie Speidel. Non-rigid volume to surface registration using a data-driven biomechanical model. In *International Conference on Medical Image Computing and Computer-Assisted Intervention*, pages 724–734. Springer, 2020. URL [https://gitlab.com/nct\\_tso\\_public/Volume2SurfaceCNN](https://gitlab.com/nct_tso_public/Volume2SurfaceCNN).
  - [32] Logan W Clements, Prashanth Dumpuri, William C Chapman, Robert L Galloway, and Michael I Miga. Atlas-based method for model updating in image-guided liver surgery. In *Medical Imaging 2007: Visualization and Image-Guided Procedures*, volume 6509, pages 424–435. SPIE, 2007.
  - [33] Zixin Yang, Richard Simon, Kelly Merrell, Cristian Linte, et al. Boundary constraint-free biomechanical model-based surface matching for intraoperative liver deformation

- correction. *arXiv preprint arXiv:2403.09964*, 2024.
- [34] Zhe Min, Zachary MC Baum, Shaheer U Saeed, Mark Emberton, Dean C Barratt, Zeike A Taylor, and Yipeng Hu. Non-rigid medical image registration using physics-informed neural networks. In *International Conference on Information Processing in Medical Imaging*, pages 601–613. Springer, 2023.
- [35] Stefan Suwelack, Sebastian Röhl, Sebastian Bodenstedt, Daniel Reichard, Rüdiger Dillmann, Thiago dos Santos, Lena Maier-Hein, Martin Wagner, Josephine Wünscher, Hannes Kenngott, et al. Physics-based shape matching for intraoperative image guidance. *Medical Physics*, 41(11):111901, 2014. URL <https://opencas.webarchiv.kit.edu/?q=PhysicsBasedShapeMatching>.
- [36] Benoit Dagon, Charles Baur, and Vincent Bettschart. A framework for intraoperative update of 3d deformable models in liver surgery. In *International Conference of the IEEE Engineering in Medicine and Biology Society*, pages 3235–3238. IEEE, 2008.
- [37] Ivan F Costa. A novel deformation method for fast simulation of biological tissue formed by fibers and fluid. *Medical Image Analysis*, 16(5):1038–1046, 2012.
- [38] C Schneider, S Thompson, J Totz, Y Song, M Allam, MH Sodergren, AE Desjardins, D Barratt, S Ourselin, K Gurusamy, et al. Comparison of manual and semi-automatic registration in augmented reality image-guided liver surgery: A clinical feasibility study. *Surgical Endoscopy*, 34:4702–4711, 2020.
- [39] Long Chen, Xin Zhang, Yuhao He, Wencong Wang, Fengfeng Zhang, and Lining Sun. A method of 3d-3d multi-stage non-rigid registration of the spine based on binocular structured light. *The International Journal of Medical Robotics and Computer Assisted Surgery*, 17(4):e2283, 2021.
- [40] Bogdan Mihai Maris and Paolo Fiorini. Deformable surface registration for breast tumors tracking: A phantom study. In *International Conference on Biomedical Engineering*, pages 20–25. IEEE, 2017.
- [41] Longfei Ma, Hanying Liang, Boxuan Han, Shizhong Yang, Xinran Zhang, and Hongen Liao. Augmented reality navigation with ultrasound-assisted point cloud registration for percutaneous ablation of liver tumors. *International Journal of Computer Assisted Radiology and Surgery*, 17(9):1543–1552, 2022.
- [42] YC Fung. Structure and stress-strain relationship of soft tissues. *American Zoologist*, 24(1):13–22, 1984.
- [43] Christoph Jud, Philippe C Cattin, and Frank Preiswerk. Statistical respiratory models for motion estimation. In *Statistical Shape and Deformation Analysis*, pages 379–407. Elsevier, 2017.
- [44] Martin von Siebenthal, Gabor Szekely, Urs Gamper, Peter Boesiger, Antony Lomax, and Ph Cattin. 4d mr imaging of respiratory organ motion and its variability. *Physics in Medicine & Biology*, 52(6):1547, 2007.
- [45] Daniel Rueckert, Luke I Sonoda, Carmel Hayes, Derek LG Hill, Martin O Leach, and David J Hawkes. Nonrigid registration using free-form deformations: Application to breast mr images. *IEEE Transactions on Medical Imaging*, 18(8):712–721, 1999.
- [46] Marc Modat, Gerard R Ridgway, Zeike A Taylor, Manja Lehmann, Josephine Barnes, David J Hawkes, Nick C Fox, and Sébastien Ourselin. Fast free-form deformation using graphics processing units. *Computer Methods and Programs in Biomedicine*, 98(3):278–284, 2010.
- [47] Yuening Wang, Ying Sun, Kexin Gan, Jie Yuan, Hanzi Xu, Han Gao, and Xiuming Zhang. Bone marrow sparing oriented multi-model image registration in cervical cancer radiotherapy. *Computers in Biology and Medicine*, 166:107581, 2023.
- [48] Andrea Mendizabal, Pablo Márquez-Neila, and Stéphane Cotin. Simulation of hyper-elastic materials in real-time using deep learning. *Medical Image Analysis*, 59:101569, 2020.
- [49] Mathieu Labrunie, Daniel Pizarro, Christophe Tilmant, and Adrien Bartoli. Automatic 3d/2d deformable registration in minimally invasive liver resection using a mesh recovery network. In *Medical Imaging with Deep Learning*, 2023. URL <https://proceedings>.



- [mlr.press/v227/labrunie24a.html](https://mlr.press/v227/labrunie24a.html).
- [50] Suraj Pawar, Omer San, Burak Aksoylu, Adil Rasheed, and Trond Kvamsdal. Physics guided machine learning using simplified theories. *Physics of Fluids*, 33(1), 2021.
  - [51] Jon S Heiselman, Jarrod A Collins, Morgan J Ringel, T Peter Kingham, William R Jarnagin, and Michael I Miga. The image-to-physical liver registration sparse data challenge: Comparison of state-of-the-art using a common dataset. *Journal of Medical Imaging*, 11(1):015001–015001, 2024. URL <https://doi.org/10.1117/1.JMI.11.1.015001>.
  - [52] Stéphanie Marchesseau, Simon Chatelin, and Hervé Delingette. Nonlinear biomechanical model of the liver. In *Biomechanics of Living Organs*, pages 243–265. Elsevier, 2017.
  - [53] Ishita Chen, Aaron M Coffey, Siyi Ding, Prashanth Dumpuri, Benoit M Dawant, Reid C Thompson, and Michael I Miga. Intraoperative brain shift compensation: Accounting for dural septa. *IEEE Transactions on Biomedical Engineering*, 58(3):499–508, 2010.
  - [54] Ishita Chen, Rowena E Ong, Amber L Simpson, Kay Sun, Reid C Thompson, and Michael I Miga. Integrating retraction modeling into an atlas-based framework for brain shift prediction. *IEEE Transactions on Biomedical Engineering*, 60(12):3494–3504, 2013.
  - [55] Jon S Heiselman, Logan W Clements, Jarrod A Collins, Jared A Weis, Amber L Simpson, Sunil K Geevarghese, T Peter Kingham, William R Jarnagin, and Michael I Miga. Characterization and correction of intraoperative soft tissue deformation in image-guided laparoscopic liver surgery. *Journal of Medical Imaging*, 5(2):021203–021203, 2018.
  - [56] Manolis IA Lourakis et al. A brief description of the levenberg-marquardt algorithm implemented by levmar. *Foundation of Research and Technology*, 4(1):1–6, 2005.
  - [57] Renzo Phellan, Bahe Hachem, Julien Clin, Jean-Marc Mac-Thiong, and Luc Duong. Real-time biomechanics using the finite element method and machine learning: Review and perspective. *Medical Physics*, 48(1):7–18, 2021.
  - [58] Siamak Niroomandi, David González, Iciar Alfaro, Felipe Bordeu, Adrien Leygue, Elías Cueto, and Francisco Chinesta. Real-time simulation of biological soft tissues: A pgd approach. *International Journal for Numerical Methods in Biomedical Engineering*, 29(5):586–600, 2013.
  - [59] Jiahua Zhu, Yixian Su, Ziteng Liu, Bainan Liu, Yu Sun, Wenpeng Gao, and Yili Fu. Real-time biomechanical modelling of the liver using lightgbm model. *The International Journal of Medical Robotics and Computer Assisted Surgery*, 18(6):e2433, 2022.
  - [60] Shaheer U Saeed, Zeike A Taylor, Mark A Pinnock, Mark Emberton, Dean C Barratt, and Yipeng Hu. Prostate motion modelling using biomechanically-trained deep neural networks on unstructured nodes. In *International Conference on Medical Image Computing and Computer-Assisted Intervention*, pages 650–659. Springer, 2020.
  - [61] Jean-Nicolas Brunet, Andrea Mendizabal, Antoine Petit, Nicolas Golse, Eric Vibert, and Stéphane Cotin. Physics-based deep neural network for augmented reality during liver surgery. In *International Conference on Medical Image Computing and Computer-Assisted Intervention*, pages 137–145. Springer, 2019.
  - [62] Micha Pfeiffer, Carina Riediger, Jürgen Weitz, and Stefanie Speidel. Learning soft tissue behavior of organs for surgical navigation with convolutional neural networks. *International Journal of Computer Assisted Radiology and Surgery*, 14:1147–1155, 2019. URL [https://gitlab.com/nct\\_tso\\_public/cnn-deformation-estimation](https://gitlab.com/nct_tso_public/cnn-deformation-estimation).
  - [63] Francisco Martínez-Martínez, María J Rupérez-Moreno, Marcelino Martínez-Sober, Juan Antonio Solves-Llorens, Delia Lorente, AJ Serrano-López, Sandra Martínez-Sanchis, C Monserrat, and José David Martín-Guerrero. A finite element-based machine learning approach for modeling the mechanical behavior of the breast tissues under compression in real-time. *Computers in Biology and Medicine*, 90:116–124, 2017.
  - [64] Oscar J Pellicer-Valero, María José Rupérez, Sandra Martínez-Sanchis, and José D Martín-Guerrero. Real-time biomechanical modeling of the liver using machine learning models trained on finite element method simulations. *Expert Systems with Applications*, 143:113083, 2020.
  - [65] Delia Lorente, Francisco Martínez-Martínez, María José Rupérez, MA Lago, Marcelino

- Martínez-Sober, Pablo Escandell-Montero, José María Martínez-Martínez, Sandra Martínez-Sanchis, Antonio J Serrano-López, C Monserrat, et al. A framework for modelling the biomechanical behaviour of the human liver during breathing in real time using machine learning. *Expert Systems with Applications*, 71:342–357, 2017.
- [66] Timothy J Carter, Maxime Sermesant, David M Cash, Dean C Barratt, Christine Tanner, and David J Hawkes. Application of soft tissue modelling to image-guided surgery. *Medical Engineering & Physics*, 27(10):893–909, 2005.
- [67] Rosalie Plantefeve, Igor Peterlik, Nazim Haouchine, and Stéphane Cotin. Patient-specific biomechanical modeling for guidance during minimally-invasive hepatic surgery. *Annals of Biomedical Engineering*, 44:139–153, 2016.
- [68] Kevin Lister, Zhan Gao, and Jaydev P Desai. Development of in vivo constitutive models for liver: Application to surgical simulation. *Annals of Biomedical Engineering*, 39:1060–1073, 2011.
- [69] Rosalie Plantefeve, Igor Peterlik, Hadrien Courtecuisse, Raffaella Trivisonne, Jean-Pierre Radoux, and Stéphane Cotin. Atlas-based transfer of boundary conditions for biomechanical simulation. In *International Conference on Medical Image Computing and Computer-Assisted Intervention*, pages 33–40. Springer, 2014.
- [70] Megumi Nakao, Mitsuhiro Nakamura, and Tetsuya Matsuda. Image-to-graph convolutional network for 2d/3d deformable model registration of low-contrast organs. *IEEE Transactions on Medical Imaging*, 41(12):3747–3761, 2022. URL <https://github.com/meguminakao/IGCN>.
- [71] Olaf Ronneberger, Philipp Fischer, and Thomas Brox. U-net: Convolutional networks for biomedical image segmentation. In *International Conference on Medical Image Computing and Computer-Assisted Intervention*, pages 234–241. Springer, 2015.
- [72] Thomas N. Kipf and Max Welling. Semi-supervised classification with graph convolutional networks. In *International Conference on Learning Representations*. OpenReview.net, 2017.
- [73] Eleonora Tagliabue, Marco Piccinelli, Diego Dall’Alba, Juan Verde, Micha Pfeiffer, Riccardo Marin, Stefanie Speidel, Paolo Fiorini, and Stéphane Cotin. Intra-operative update of boundary conditions for patient-specific surgical simulation. In *International Conference on Medical Image Computing and Computer-Assisted Intervention*, pages 373–382. Springer, 2021. URL <https://gitlab.com/altairLab/banet>.
- [74] Eleonora Tagliabue, Diego Dall’Alba, Micha Pfeiffer, Marco Piccinelli, Riccardo Marin, Umberto Castellani, Stefanie Speidel, and Paolo Fiorini. Data-driven intra-operative estimation of anatomical attachments for autonomous tissue dissection. *IEEE Robotics and Automation Letters*, 6(2):1856–1863, 2021.
- [75] Kaiming He, Xiangyu Zhang, Shaoqing Ren, and Jian Sun. Deep residual learning for image recognition. In *Proceedings of the IEEE conference on Computer Vision and Pattern Recognition*, pages 770–778. IEEE, 2016.
- [76] Joao Carreira, Pulkit Agrawal, Katerina Fragkiadaki, and Jitendra Malik. Human pose estimation with iterative error feedback. In *Proceedings of the IEEE conference on Computer Vision and Pattern Recognition*, pages 4733–4742. IEEE, 2016.
- [77] Satya N Atluri, JY Cho, and H-G Kim. Analysis of thin beams, using the meshless local petrov–galerkin method, with generalized moving least squares interpolations. *Computational Mechanics*, 24(5):334–347, 1999.
- [78] Meng Jia and Matthew Kyan. Learning occupancy function from point clouds for surface reconstruction. *arXiv preprint arXiv:2010.11378*, 2020.
- [79] D Caleb Rucker, Yifei Wu, Logan W Clements, Janet E Ondrake, Thomas S Pfeiffer, Amber L Simpson, William R Jarnagin, and Michael I Miga. A mechanics-based nonrigid registration method for liver surgery using sparse intraoperative data. *IEEE Transactions on Medical Imaging*, 33(1):147–158, 2013.
- [80] Rui Wang and Rose Yu. Physics-guided deep learning for dynamical systems: A survey. *arXiv preprint arXiv:2107.01272*, 2021.
- [81] Charles R Qi, Hao Su, Kaichun Mo, and Leonidas J Guibas. Pointnet: Deep learning

- on point sets for 3d classification and segmentation. In *Proceedings of the IEEE/CVF Conference on Computer Vision and Pattern Recognition*, pages 652–660, 2017.
- [82] Guillaume Mestdagh and Stéphane Cotin. An optimal control problem for elastic registration and force estimation in augmented surgery. In *International Conference on Medical Image Computing and Computer-Assisted Intervention*, pages 74–83. Springer, 2022.
- [83] Morgan Ringel, Jon Heiselman, Winona Richey, Ingrid Meszoely, William Jarnagin, and Michael Miga. Comparing regularized kelvinlet functions and the finite element method for registration of medical images to sparse organ data. *arXiv preprint arXiv:2306.05509*, 2023.
- [84] Mohammad Karami, Hervé Lombaert, and David Rivest-Hénault. Real-time simulation of viscoelastic tissue behavior with physics-guided deep learning. *Computerized Medical Imaging and Graphics*, 104:102165, 2023.
- [85] Karl Ljungkvist. *Techniques for finite element methods on modern processors*. PhD thesis, Uppsala University, 2015.
- [86] Achim Schweikard, Hiroya Shiomi, and John Adler. Respiration tracking in radiosurgery. *Medical Physics*, 31(10):2738–2741, 2004.
- [87] Ruotong Li, Yuqi Tong, Tianpei Yang, Jianxi Guo, Weixin Si, Yanfang Zhang, Reinhard Klein, and Pheng-Ann Heng. Towards quantitative and intuitive percutaneous tumor puncture via augmented virtual reality. *Computerized Medical Imaging and Graphics*, 90:101905, 2021.
- [88] Yangyang Shi, Yuqi Tong, Ruotong Li, and Weixin Si. Internal motion estimation during free-breathing via external/internal correlation model. In *International Conference on Real-time Computing and Robotics*, pages 986–990. IEEE, 2021.
- [89] Ruotong Li, Weixin Si, Xiangyun Liao, Qiong Wang, Reinhard Klein, and Pheng-Ann Heng. Mixed reality based respiratory liver tumor puncture navigation. *Computational Visual Media*, 5:363–374, 2019.
- [90] SA Nicolau, Xavier Pennec, Luc Soler, and Nicholas Ayache. Clinical evaluation of a respiratory gated guidance system for liver punctures. In *International Conference on Medical Image Computing and Computer-Assisted Intervention*, pages 77–85. Springer, 2007.
- [91] Nicolas Golse, Antoine Petit, Maité Lewin, Eric Vibert, and Stéphane Cotin. Augmented reality during open liver surgery using a markerless non-rigid registration system. *Journal of Gastrointestinal Surgery*, 25:662–671, 2021.
- [92] José M González-Darder and José M González-Darder. ‘state of the art’ of the craniotomy in the early twenty-first century and future development. *Trepanation, Trephining and Craniotomy: History and Stories*, pages 421–427, 2019.
- [93] Siming Bayer, Andreas Maier, Martin Ostermeier, Rebecca Fahrig, et al. Intraoperative imaging modalities and compensation for brain shift in tumor resection surgery. *International Journal of Biomedical Imaging*, 2017, 2017.
- [94] Michael I Miga, Kay Sun, Ishita Chen, Logan W Clements, Thomas S Pheiffer, Amber L Simpson, and Reid C Thompson. Clinical evaluation of a model-updated image-guidance approach to brain shift compensation: Experience in 16 cases. *International Journal of Computer Assisted Radiology and Surgery*, 11:1467–1474, 2016.
- [95] Nazim Haouchine, Parikshit Juvekar, Alexandra Golby, William M Wells III, Stéphane Cotin, and Sarah Frisken. Alignment of cortical vessels viewed through the surgical microscope with preoperative imaging to compensate for brain shift. In *Medical Imaging 2020: Image-Guided Procedures, Robotic Interventions, and Modeling*, volume 11315, pages 478–485. SPIE, 2020.
- [96] Soumya Ghose, Jhimli Mitra, David Mills, Desmond Teck-Beng Yeo, Thomas K Foo, Alexandra Golby, and Sarah Frisken. Automatic non-rigid registration of preoperative mri and intraoperative us for us-guided neurosurgery—a preliminary study. In *International Ultrasonics Symposium*, pages 1–4. IEEE, 2021.
- [97] Nazim Haouchine, Parikshit Juvekar, Michael Necessian, William M Wells III, Alexan-

- dra Golby, and Sarah Frisken. Pose estimation and non-rigid registration for augmented reality during neurosurgery. *IEEE Transactions on Biomedical Engineering*, 69(4):1310–1317, 2021.
- [98] Nazim Haouchine, Parikshit Juvekar, William M Wells III, Stephane Cotin, Alexandra Golby, and Sarah Frisken. Deformation aware augmented reality for craniotomy using 3d/2d non-rigid registration of cortical vessels. In *International Conference on Medical Image Computing and Computer-Assisted Intervention*, pages 735–744. Springer, 2020.
- [99] D-X Zhuang, Y-X Liu, J-S Wu, C-J Yao, Y Mao, C-X Zhang, M-N Wang, W Wang, and L-F Zhou. A sparse intraoperative data-driven biomechanical model to compensate for brain shift during neuronavigation. *American Journal of Neuroradiology*, 32(2):395–402, 2011.
- [100] Winona L Richey, Jon S Heiselman, Morgan J Ringel, Ingrid M Meszoely, and Michael I Miga. Computational imaging to compensate for soft-tissue deformations in image-guided breast conserving surgery. *IEEE Transactions on Biomedical Engineering*, 69(12):3760–3771, 2022.
- [101] Sandro Ferrari, Eleonora Tagliabue, Bogdan Mihai Maris, and Paolo Fiorini. Autonomous robotic system for breast biopsy with deformation compensation. *IEEE Robotics and Automation Letters*, 8(3):1215–1222, 2023.
- [102] Mehran Ebrahimi, Peter Siegler, Amen Modhafar, Claire MB Holloway, Donald B Plewes, and Anne L Martel. Using surface markers for mri guided breast conserving surgery: A feasibility survey. *Physics in Medicine & Biology*, 59(7):1589, 2014.
- [103] Timothy Y Wang, Farah Hamouda, Eric W Sankey, Vikram A Mehta, Chester K Yarbrough, and Muhammad M Abd-El-Barr. Computer-assisted instrument navigation versus conventional c-arm fluoroscopy for surgical instrumentation: Accuracy, radiation time, and radiation exposure. *American Journal of Roentgenology*, 213(3):651–658, 2019.
- [104] Masato Tanaka, Yoshihiro Fujiwara, Koji Uotani, Vijay Kamath, Taro Yamauchi, and Hisanori Ikuma. Percutaneous transdiscal pedicle screw fixation for osteoporotic vertebral fracture: A technical note. *Interdisciplinary Neurosurgery*, 23:100903, 2021.
- [105] Shaoyi Du, Chunjia Zhang, Zongze Wu, Juan Liu, and Jianru Xue. Robust isotropic scaling icp algorithm with bidirectional distance and bounded rotation angle. *Neurocomputing*, 215:160–168, 2016.
- [106] Siyeop Yoon, Chang Hwan Yoon, and Deukhee Lee. Topological recovery for non-rigid 2d/3d registration of coronary artery models. *Computer Methods and Programs in Biomedicine*, 200:105922, 2021.
- [107] Jianjun Zhu, Heng Li, Danni Ai, Qi Yang, Jingfan Fan, Yong Huang, Hong Song, Yechen Han, and Jian Yang. Iterative closest graph matching for non-rigid 3d/2d coronary arteries registration. *Computer Methods and Programs in Biomedicine*, 199:105901, 2021.
- [108] Pascal Haigron, Aurélien Dumenil, Adrien Kaladji, Michel Rochette, B Bou Said, Simon Esneault, Hélène Walter-Le Berre, Ghizlane Mouktadiri, Miguel Castro, Pierre Louat, et al. Angiovision: Aortic stent-graft placement by augmented angionavigation. *IRBM*, 34(2):167–175, 2013.
- [109] Sidaty El Hadramy, Juan Verde, Nicolas Padoy, and Stéphane Cotin. Intraoperative ct augmentation for needle-based liver interventions. In *International Conference on Medical Image Computing and Computer-Assisted Intervention*, pages 291–301. Springer, 2023.
- [110] Jaime Garcia Guevara, Igor Peterlik, Marie-Odile Berger, and Stéphane Cotin. Elastic registration based on compliance analysis and biomechanical graph matching. *Annals of Biomedical Engineering*, 48:447–462, 2020.
- [111] Maxime Gérard, François Michaud, Alexandre Bigot, An Tang, Gilles Soulez, and Samuel Kadoury. Geometric modeling of hepatic arteries in 3d ultrasound with unsupervised mra fusion during liver interventions. *International Journal of Computer Assisted Radiology and Surgery*, 12:961–972, 2017.
- [112] Masoud S Nosrati, Rafeef Abugharbieh, Jean-Marc Peyrat, Julien Abinahed, Osama Al-Alao, Abdulla Al-Ansari, and Ghassan Hamarneh. Simultaneous multi-structure

- segmentation and 3d nonrigid pose estimation in image-guided robotic surgery. *IEEE Transactions on Medical Imaging*, 35(1):1–12, 2015.
- [113] Christoph J Paulus, Nazim Haouchine, Seong-Ho Kong, Renato Vianna Soares, David Cazier, and Stéphane Cotin. Handling topological changes during elastic registration: Application to augmented reality in laparoscopic surgery. *International Journal of Computer Assisted Radiology and Surgery*, 12:461–470, 2017.
- [114] Xiaohui Zhang, Junchen Wang, Tianmiao Wang, Xuquan Ji, Yu Shen, Zhen Sun, and Xuebin Zhang. A markerless automatic deformable registration framework for augmented reality navigation of laparoscopy partial nephrectomy. *International Journal of Computer Assisted Radiology and Surgery*, 14:1285–1294, 2019.
- [115] Jasper N Smit, Koert FD Kuhlmann, Bart R Thomson, Niels FM Kok, Theo JM Ruers, and Matteo Fusaglia. Ultrasound guidance in navigated liver surgery: toward deep-learning enhanced compensation of deformation and organ motion. *International Journal of Computer Assisted Radiology and Surgery*, 19(1):1–9, 2024.
- [116] Max Allan, Ankur Kapoor, Philip Mewes, and Peter Mountney. Non rigid registration of 3d images to laparoscopic video for image guided surgery. In *Computer-Assisted and Robotic Endoscopy*, pages 109–116. Springer, 2016.
- [117] Yanying Zhang, Wenguo Hou, et al. Non-rigid registration with volumetric mesh for liver surgery.
- [118] Chengfeng Sun, Peng Li, Xiaojun Wu, Xing Gao, and Yunhui Liu. Research on manipulation of soft tissue based on 3d vision. In *International Conference on Cyborg and Bionic Systems*, pages 374–379. IEEE, 2023.
- [119] Haocheng Huang, Zhengyan Zhang, Zhe Min, Max Q-H Meng, Shuang Song, and Jiaole Wang. Non-rigid 3d point set registration with reliable hybrid mixture model. In *International Conference on Robotics and Biomimetics*, pages 1–6. IEEE, 2023.
- [120] Bu Xu, Lu Wang, Jinzhong Yang, Benqiang Yang, Lisheng Xu, Yang Chen, and Dingchang Zheng. Multi-constraint point set registration with redundant point removal for the registration of coronary arteries. *Computers in Biology and Medicine*, 165:107438, 2023. URL <https://github.com/abcxubu/Dataset-of-vascular-tree-point-set>.
- [121] Jingwei Song, Keke Yang, Zheng Zhang, Meng Li, Tuoyu Cao, and Maani Ghaffari. Iterative pnp and its application in 3d-2d vascular image registration for robot navigation. *arXiv preprint arXiv:2310.12551*, 2023.
- [122] Jianjun Zhu, Cheng Wang, Yi Zhang, Meixiao Zhan, Wei Zhao, Sitong Teng, Ligong Lu, and Gao-Jun Teng. 3d/2d vessel registration based on monte carlo tree search and manifold regularization. *IEEE Transactions on Medical Imaging*, 2023. URL [https://github.com/JianjunZhu/Vessel\\_3D\\_2D\\_Registration](https://github.com/JianjunZhu/Vessel_3D_2D_Registration).
- [123] Fang Chen, Xiwen Cui, Boxuan Han, Jia Liu, Xinran Zhang, and Hongen Liao. Augmented reality navigation for minimally invasive knee surgery using enhanced arthroscopy. *Computer Methods and Programs in Biomedicine*, 201:105952, 2021.
- [124] Jong-Ha Lee, Chang-Hee Won, and Nathaniel Marchetti. Determining the operative line of resection for image-guided emphysema surgery using a laser scanner and non-rigid registration. *The International Journal of Medical Robotics and Computer Assisted Surgery*, 6(2):239–249, 2010.
- [125] Thomas Lange, Sebastian Eulenstein, Michael Hünerbein, Hans Lamecker, and Peter-Michael Schlag. Augmenting intraoperative 3d ultrasound with preoperative models for navigation in liver surgery. In *International Conference on Medical Image Computing and Computer-Assisted Intervention*, pages 534–541. Springer, 2004.
- [126] Morgan Ringel, Jon Heiselman, Winona Richey, Ingrid Meszoely, and Michael Miga. Regularized kelinlet functions to model linear elasticity for image-to-physical registration of the breast. In *International Conference on Medical Image Computing and Computer-Assisted Intervention*, pages 344–353. Springer, 2023.
- [127] Yinoussa Adagolodjo, Nicolas Golse, Eric Vibert, Michel De Mathelin, Stéphane Cotin, and Hadrien Courtecuisse. Marker-based registration for large deformations-application to open liver surgery. In *International Conference on Robotics and Automation*, pages

- 4007–4012. IEEE, 2018.
- [128] Jarrod A Collins, Jared A Weis, Jon S Heiselman, Logan W Clements, Amber L Simpson, William R Jarnagin, and Michael I Miga. Improving registration robustness for image-guided liver surgery in a novel human-to-phantom data framework. *IEEE Transactions on Medical Imaging*, 36(7):1502–1510, 2017.
- [129] Yamid Espinel, Erol Özgür, Lilian Calvet, Bertrand Le Roy, Emmanuel Buc, and Adrien Bartoli. Combining visual cues with interactions for 3d–2d registration in liver laparoscopy. *Annals of Biomedical Engineering*, 48:1712–1727, 2020.
- [130] Hugo Jobidon-Lavergne, Samuel Kadoury, Dejan Knez, and Carl-Éric Aubin. Biomechanically driven intraoperative spine registration during navigated anterior vertebral body tethering. *Physics in Medicine & Biology*, 64(11):115008, 2019.
- [131] Yinoussa Adagolodjo, Raffaella Trivisonne, Nazim Haouchine, Stéphane Cotin, and Hadrien Courtecuisse. Silhouette-based pose estimation for deformable organs application to surgical augmented reality. In *International Conference on Intelligent Robots and Systems*, pages 539–544. IEEE, 2017.
- [132] Nazim Haouchine, Stephane Cotin, Igor Peterlik, Jeremie Dequidt, Mario Sanz Lopez, Erwan Kerrien, and Marie-Odile Berger. Impact of soft tissue heterogeneity on augmented reality for liver surgery. *IEEE Transactions on Visualization and Computer Graphics*, 21(5):584–597, 2014.
- [133] Seong-Ho Kong, Nazim Haouchine, Renato Soares, Andrey Klymchenko, Bohdan Andreiuk, Bruno Marques, Galyna Shabat, Thierry Piechaud, Michele Diana, Stéphane Cotin, et al. Robust augmented reality registration method for localization of solid organs’ tumors using ct-derived virtual biomechanical model and fluorescent fiducials. *Surgical Endoscopy*, 31:2863–2871, 2017.
- [134] Esther Wild, Dogu Teber, Daniel Schmid, Tobias Simpfendörfer, Michael Müller, Ann-Christin Baranski, Hannes Kenngott, Klaus Kopka, and Lena Maier-Hein. Robust augmented reality guidance with fluorescent markers in laparoscopic surgery. *International Journal of Computer Assisted Radiology and Surgery*, 11:899–907, 2016.
- [135] Nazim Haouchine, Frederick Roy, Lionel Untereiner, and Stéphane Cotin. Using contours as boundary conditions for elastic registration during minimally invasive hepatic surgery. In *International Conference on Intelligent Robots and Systems*, pages 495–500. IEEE, 2016.
- [136] Yifei Wu, D Caleb Rucker, Rebekah H Conley, Thomas S Pheiffer, Amber L Simpson, Sunil K Geevarghese, and Michael I Miga. Registration of liver images to minimally invasive intraoperative surface and subsurface data. In *Medical Imaging 2014: Image-Guided Procedures, Robotic Interventions, and Modeling*, volume 9036, pages 228–235. SPIE, 2014.
- [137] Nazim Haouchine, Jérémie Dequidt, Marie-Odile Berger, and Stéphane Cotin. Deformation-based augmented reality for hepatic surgery. *Studies in Health Technology and Informatics*, 184, 2013.
- [138] Bruno Marques, Rosalie Plantefève, Frédérick Roy, Nazim Haouchine, Emmanuel Jeanvoine, Igor Peterlik, and Stéphane Cotin. Framework for augmented reality in minimally invasive laparoscopic surgery. In *International conference on E-health Networking, Application & Services*, pages 22–27. IEEE, 2015.
- [139] Nazim Haouchine, Jérémie Dequidt, Erwan Kerrien, Marie-Odile Berger, and Stéphane Cotin. Physics-based augmented reality for 3d deformable object. In *Workshop on Virtual Reality Interaction and Physical Simulation*. The Eurographics Association, 2012.
- [140] Amrollah Mohammadi, Alireza Ahmadian, Amir Darbandi Azar, Ahmad Darban Sheykh, Faramarz Amiri, and Javad Alirezaie. Estimation of intraoperative brain shift by combination of stereovision and doppler ultrasound: Phantom and animal model study. *International Journal of Computer Assisted Radiology and Surgery*, 10:1753–1764, 2015.
- [141] Thomas S Pheiffer, Reid C Thompson, Daniel C Rucker, Amber L Simpson, and Michael I Miga. Model-based correction of tissue compression for tracked ultrasound in soft tissue image-guided surgery. *Ultrasound in Medicine & Biology*, 40(4):788–803,

- 2014.
- [142] Xiaoyao Fan, Songbai Ji, Alex Hartov, David Roberts, and Keith Paulsen. Retractor-induced brain shift compensation in image-guided neurosurgery. In *Medical Imaging 2013: Image-Guided Procedures, Robotic Interventions, and Modeling*, volume 8671, pages 150–157. SPIE, 2013.
  - [143] Rebekah H Conley, Ingrid M Meszoely, Jared A Weis, Thomas S Pheiffer, Lori R Arlinghaus, Thomas E Yankeelov, and Michael I Miga. Realization of a biomechanical model-assisted image guidance system for breast cancer surgery using supine mri. *International Journal of Computer Assisted Radiology and Surgery*, 10:1985–1996, 2015.
  - [144] Tim Carter, Lianghao Han, Zeike Taylor, Christine Tanner, Nick Beechy-Newman, Sébastien Ourselin, and David Hawkes. Application of biomechanical modelling to image-guided breast surgery. *Soft Tissue Biomechanical Modeling for Computer Assisted Surgery*, pages 71–94, 2012.
  - [145] Siavash Khallaghi, C Antonio Sánchez, Abtin Rasouljan, Yue Sun, Farhad Imani, Amir Khojaste, Orcun Goksel, Cesare Romagnoli, Hamidreza Abdi, Silvia Chang, et al. Biomechanically constrained surface registration: Application to mr-trus fusion for prostate interventions. *IEEE Transactions on Medical Imaging*, 34(11):2404–2414, 2015. URL <https://github.com/siavashk/GMM-FEM>.
  - [146] Andriy Fedorov, Siavash Khallaghi, C Antonio Sánchez, Andras Lasso, Sidney Fels, Kemal Tuncali, Emily Neubauer Sugar, Tina Kapur, Chenxi Zhang, William Wells, et al. Open-source image registration for mri–trus fusion-guided prostate interventions. *International Journal of Computer Assisted Radiology and Surgery*, 10:925–934, 2015. URL <https://github.com/siavashk/GMM-FEM>.
  - [147] Peter Mountney, Johannes Fallert, Stephane Nicolau, Luc Soler, and Philip W Mewes. An augmented reality framework for soft tissue surgery. In *International Conference on Medical Image Computing and Computer-Assisted Intervention*, pages 423–431. Springer, 2014.
  - [148] Benjamin Berkels, Sebastian Bauer, Svenja Ettl, Oliver Arold, Joachim Hornegger, and Martin Rumpf. Joint surface reconstruction and 4d deformation estimation from sparse data and prior knowledge for marker-less respiratory motion tracking. *Medical Physics*, 40(9):091703, 2013.
  - [149] Min Li, Edward Castillo, Xiao-Lin Zheng, Hong-Yan Luo, Richard Castillo, Yi Wu, and Thomas Guerrero. Modeling lung deformation: A combined deformable image registration method with spatially varying young’s modulus estimates. *Medical Physics*, 40(8):081902, 2013.
  - [150] Fenghong Liu, Keith D Paulsen, Alexander Hartov, and David W Roberts. A surface misfit inversion method for brain deformation modeling. In *Medical Imaging 2007: Visualization and Image-Guided Procedures*, volume 6509, pages 892–899. SPIE, 2007.
  - [151] Marek Bucki, Claudio Lobos, and Yohan Payan. Framework for a low-cost intra-operative image-guided neuronavigator including brain shift compensation. In *International Conference of the IEEE Engineering in Medicine and Biology Society*, pages 872–875. IEEE, 2007.
  - [152] Adam Wittek, Ron Kikinis, Simon K Warfield, and Karol Miller. Brain shift computation using a fully nonlinear biomechanical model. In *International Conference on Medical Image Computing and Computer-Assisted Intervention*, pages 583–590. Springer, 2005.
  - [153] Prashanth Dumpuri, Logan W Clements, Benoit M Dawant, and Michael I Miga. Model-updated image-guided liver surgery: Preliminary results using surface characterization. *Progress in Biophysics and Molecular Biology*, 103(2-3):197–207, 2010.
  - [154] David M Cash, Michael I Miga, Sean C Glasgow, Benoit M Dawant, Logan W Clements, Zhujiang Cao, Robert L Galloway, and William C Chapman. Concepts and preliminary data toward the realization of image-guided liver surgery. *Journal of Gastrointestinal Surgery*, 11:844–859, 2007.
  - [155] Aziliz Guezou-Philippe, Guillaume Dardenne, Hoel Letissier, Agathe Yvinou, Valérie Burdin, Eric Stindel, and Christian Lefèvre. Anterior pelvic plane estimation for total



- hip arthroplasty using a joint ultrasound and statistical shape model based approach. *Medical & Biological Engineering & Computing*, 61(1):195–204, 2023.
- [156] Xiao-Yun Zhou, Guang-Zhong Yang, and Su-Lin Lee. A real-time and registration-free framework for dynamic shape instantiation. *Medical Image Analysis*, 44:86–97, 2018.
- [157] Yan Hu, Jun Wei, Tianmiao Wang, Qinjun Zhao, Honghua Zhao, and Shi Li. 3d morphing method based on kriging algorithm for surgical navigation. In *34th Chinese Control Conference*, pages 8372–8376. IEEE, 2015.
- [158] Qiong Han, Stephen E Strup, Melody C Carswell, Duncan Clarke, and Williams B Seales. Model completion via deformation cloning based on an explicit global deformation model. In *International Conference on Medical Image Computing and Computer-Assisted Intervention*, pages 1067–1074. Springer, 2009.
- [159] Long Chen, Li Ma, Fengfeng Zhang, Wei Zhan, Xinrong Yang, and Lining Sun. A method of three-dimensional non-rigid localization of liver tumors based on structured light. *Optics and Lasers in Engineering*, 174:107962, 2024.
- [160] Fei Liu, Zihan Li, Yunhai Han, Jingpei Lu, Florian Richter, and Michael C Yip. Real-to-sim registration of deformable soft tissue with position-based dynamics for surgical robot autonomy. In *International Conference on Robotics and Automation*, pages 12328–12334. IEEE, 2021.
- [161] Dingrong Wang, Soheil Azadvar, Jon Heiselman, Xiajun Jiang, Michael Miga, and Linwei Wang. Libr+: Improving intraoperative liver registration by learning the residual of biomechanics-based deformable registration. *arXiv preprint arXiv:2403.06901*, 2024.
- [162] Andrea Mendizabal, Eleonora Tagliabue, and Diego Dall’Alba. Intraoperative estimation of liver boundary conditions from multiple partial surfaces. *International Journal of Computer Assisted Radiology and Surgery*, 18(7):1295–1302, 2023. URL <https://gitlab.com/altairLab/banet/-/tree/banet2.0>.
- [163] Ho-Gun Ha, Jinhan Lee, Gu-Hee Jung, Jaesung Hong, and HyunKi Lee. 2d-3d reconstruction of a femur by single x-ray image based on deep transfer learning network. *IRBM*, 45(1):100822, 2024.
- [164] Florentin Liebmann, Marco von Atzigen, Dominik Stütz, Julian Wolf, Lukas Zingg, Daniel Suter, Nicola A Cavalcanti, Laura Leoty, Hooman Esfandiari, Jess G Snedeker, et al. Automatic registration with continuous pose updates for marker-less surgical navigation in spine surgery. *Medical Image Analysis*, 91:103027, 2024.
- [165] Xiao Zhang, Feihong Liu, Yuning Gu, Xiaosong Xiong, Caiwen Jiang, Jun Feng, and Dinggang Shen. Spr-net: Structural points based registration for coronary arteries across systolic and diastolic phases. In *International Conference on Medical Image Computing and Computer-Assisted Intervention*, pages 791–801. Springer, 2023.
- [166] Long Lei, Li Huang, Baoliang Zhao, Ying Hu, Zhongliang Jiang, Jianwei Zhang, and Bing Li. Diffeomorphic respiratory motion estimation of thoracoabdominal organs for image-guided interventions. *Medical Physics*, 48(8):4160–4176, 2021.
- [167] Shirin Shakeri, William Le, Cynthia Ménard, and Samuel Kadoury. Deformable mri to transrectal ultrasound registration for prostate interventions with shape-based deep variational auto-encoders. In *International Symposium on Biomedical Imaging*, pages 174–178. IEEE, 2021.
- [168] Alban Odot, Guillaume Mestdagh, Yannick Privat, and Stéphane Cotin. Real-time elastic partial shape matching using a neural network-based adjoint method. In *International Conference on Optimization and Learning*, pages 137–147. Springer, 2023.
- [169] Yasmin Salehi and Dennis Giannacopoulos. Physgcn: A physics-driven graph neural network based model for predicting soft tissue deformation in image-guided neurosurgery. *Advances in Neural Information Processing Systems*, 35:37282–37296, 2022. URL <https://github.com/YasminSalehi/PhysGNN>.
- [170] Sidaty El, Juan Verde, Nicolas Padoy, and Stéphane Cotin. Towards real-time vessel guided augmented reality for liver surgery. 2024.
- [171] Mohammad Farid Azampour, Maria Tirindelli, Jane Lameski, Miruna Gafencu, Eleonora Tagliabue, Emad Fatemizadeh, Ilker Hacihaliloglu, and Nassir Navab. Anatomy-aware

- computed tomography-to-ultrasound spine registration. *Medical Physics*, 2023. URL [https://github.com/mfazampour/medphys\\_ct\\_us\\_registration](https://github.com/mfazampour/medphys_ct_us_registration).
- [172] Michael Young, Zixin Yang, Richard Simon, and Cristian A Linte. Investigating transformer encoding techniques to improve data-driven volume-to-surface liver registration for image-guided navigation. In *MICCAI Workshop on Data Engineering in Medical Imaging*, pages 91–101. Springer, 2023.
- [173] Hua-Chieh Shao, Yunxiang Li, Jing Wang, Steve Jiang, and You Zhang. Real-time liver tumor localization via combined surface imaging and a single x-ray projection. *Physics in Medicine & Biology*, 68(6):065002, 2023.
- [174] Utako Yamamoto, Megumi Nakao, Masayuki Ohzeki, Junko Tokuno, Toyofumi Fengshi Chen-Yoshikawa, and Tetsuya Matsuda. Kernel-based framework to estimate deformations of pneumothorax lung using relative position of anatomical landmarks. *Expert Systems with Applications*, 183:115288, 2021.
- [175] Navid Rabbani, Lilian Calvet, Yamid Espinel, Bertrand Le Roy, Mathieu Ribeiro, Emmanuel Buc, and Adrien Bartoli. A methodology and clinical dataset with ground-truth to evaluate registration accuracy quantitatively in computer-assisted laparoscopic liver resection. *Computer Methods in Biomechanics and Biomedical Engineering: Imaging & Visualization*, 10(4):441–450, 2022. URL [https://encov.ip.uca.fr/ab/code\\_and\\_datasets/datasets/llr\\_reg\\_evaluation\\_by\\_lus/index.php](https://encov.ip.uca.fr/ab/code_and_datasets/datasets/llr_reg_evaluation_by_lus/index.php).
- [176] Richard Modrzejewski, Toby Collins, Barbara Seeliger, Adrien Bartoli, Alexandre Hostettler, and Jacques Marescaux. An in vivo porcine dataset and evaluation methodology to measure soft-body laparoscopic liver registration accuracy with an extended algorithm that handles collisions. *International Journal of Computer Assisted Radiology and Surgery*, 14:1237–1245, 2019. URL <https://www.ircad.fr/research/data-sets/respiratory-cycle-3d-ircadb-02-copy/>.
- [177] Tonke De Jong, A (Adriaan) Moelker, J (Jenny) Dankelman, and J J (john) van den Dobbelsteen. 3D models of liver and rib cage of four patients during inspiration and expiration, 2019. URL <https://research.tudelft.nl/en/datasets/3d-models-of-liver-and-rib-cage-of-four-patients-during-inspirati>.
- [178] The respiratory cycle 3d-ircadb-02 dataset. <https://www.ircad.fr/research/data-sets/respiratory-cycle-3d-ircadb-02/>.
- [179] Sharib Ali, Yamid Espinel, Yueming Jin, Peng Liu, Bianca Güttner, Xukun Zhang, Lihua Zhang, Tom Dowrick, Matthew J Clarkson, Shiting Xiao, et al. An objective comparison of methods for augmented reality in laparoscopic liver resection by preoperative-to-intraoperative image fusion. *arXiv preprint arXiv:2401.15753*, 2024.
- [180] Taylor L Bobrow, Mayank Golhar, Rohan Vijayan, Venkata S Akshintala, Juan R Garcia, and Nicholas J Durr. Colonoscopy 3d video dataset with paired depth from 2d-3d registration. *Medical Image Analysis*, 90:102956, 2023. URL <https://durrlab.github.io/C3VD/>.
- [181] Inbar Fried, Janine Hoelscher, Jason A Akulian, and Ron Alterovitz. A dataset of anatomical environments for medical robots: Modeling respiratory deformation. 2023. URL <https://github.com/UNC-Robotics/Med-RAD>.
- [182] S Natarajan, A Priester, D Margolis, J Huang, and L Marks. Prostate mri and ultrasound with pathology and coordinates of tracked biopsy (prostate-mri-us-biopsy). *Cancer Imaging Arch*, 10:7937, 2020. URL <https://doi.org/10.7937/TCIA.2020.A61I0C1A>.
- [183] Nazim Haouchine, Jeremie Dequidt, Igor Peterlik, Erwan Kerrien, Marie-Odile Berger, and Stephane Cotin. Towards an accurate tracking of liver tumors for augmented reality in robotic assisted surgery. In *International Conference on Robotics and Automation*, pages 4121–4126. IEEE, 2014.
- [184] Rosalie Plantefeve, Nazim Haouchine, Jean-Pierre Radoux, and Stéphane Cotin. Automatic alignment of pre and intraoperative data using anatomical landmarks for augmented laparoscopic liver surgery. In *International Symposium on Biomedical Simulation*, pages 58–66. Springer, 2014.
- [185] Nazim Haouchine, Jeremie Dequidt, Igor Peterlik, Erwan Kerrien, Marie-Odile Berger,

- and Stéphane Cotin. Image-guided simulation of heterogeneous tissue deformation for augmented reality during hepatic surgery. In *International Symposium on Mixed and Augmented Reality*, pages 199–208. IEEE, 2013.
- [186] David M Cash, Michael I Miga, Tuhin K Sinha, Robert L Galloway, and William C Chapman. Compensating for intraoperative soft-tissue deformations using incomplete surface data and finite elements. *IEEE Transactions on Medical Imaging*, 24(11):1479–1491, 2005.
- [187] Yixun Liu, Andriy Fedorov, Ron Kikinis, and Nikos Chrisochoides. A novel point based non-rigid registration method and its application on brain shift. In *SPIE Medical Imaging*, 2010.
- [188] Jaime Garcia Guevara, Igor Peterlik, Marie-Odile Berger, and Stéphane Cotin. Biomechanics-based graph matching for augmented ct-cbct. *International Journal of Computer Assisted Radiology and Surgery*, 13:805–813, 2018.
- [189] Kumar T Rajamani, Martin A Styner, Haydar Talib, Guoyan Zheng, Lutz P Nolte, and Miguel A González Ballester. Statistical deformable bone models for robust 3d surface extrapolation from sparse data. *Medical Image Analysis*, 11(2):99–109, 2007.

## Appendix

**Table A.1.** The search terms used for the review process.

Sources	Search Terms	Counts
Scopus	TITLE-ABS-KEY ( ( preoperative OR pre-operative OR intra-operative OR intra-operative OR respirat* OR breath* ) AND ( model* OR organ OR *tissue ) AND ( *rigid OR deform* OR motion OR displace* ) AND ( *surg* OR laparoscop* OR endoscop* OR arthroskop* OR "Radiofrequency Ablation" OR resection OR biopsy ) AND ( navigat* OR guid* ) AND ( regist* OR align* OR correlat* ) ) AND ( LIMIT-TO ( LANGUAGE , "English" ) )	1115
Web of Science	((((((AB=(Preoperative OR Pre-operative OR Intraoperative OR Intra-operative OR Respirat* OR Breath* OR Interact*)) AND AB=(Mesh OR "Point Cloud" OR Model* OR Organ OR tissue*OR Anatom*)) AND ALL=(nonrigid OR non-rigid OR motion)) AND ALL=(Deform*))) AND AB=(surg* OR Laparoscop* OR Endoscop* OR Arthroskop* OR "Radiofrequency Ablation" OR Resection OR Biopsy)) AND ALL=(Navigat* OR Guid*)) AND ALL=(Regist* OR Correlat*)	170
IEEE Xplore	("Abstract":Preoperative OR "Abstract":Pre-operative OR "Abstract":Intraoperative OR "Abstract":Intra-operative OR "Abstract":Respirat* OR "Abstract":Breath*) AND ("Abstract":Mesh OR"Point Cloud"OR Model* OR "Abstract":*tissue* OR "Abstract":Organ OR "Abstract":Anatom*) AND ("Full Text Only":*rigid) AND ("Abstract":*surg* OR "Abstract":Laparoscop* OR "Abstract":Endoscop* OR "Abstract":Arthroskop* OR "Abstract":"Radiofrequency Ablation" OR "Abstract":Resection OR "Abstract":Biopsy) AND ("Full Text Only":Navigat* OR "Full Text Only":Guid*) AND ("Full Text Only":Regist* OR "Full Text Only":Align* OR "Full Text Only":Correlat*) AND ("Full Text Only":Deform*)	265
ScienceDirect	Find articles with these terms: (Intraoperative OR Intra-operative) AND (non-rigid OR nonrigid) AND (Deformation OR Motion) AND ( Registration OR Correlation) AND navigation Title, abstract or author-specified keywords: Surgery OR Laparoscopic OR Endoscopic OR Arthroscopic OR Ablation OR Resection OR Biopsy	338
PubMed	(((Preoperative[Title/Abstract] OR Pre-operative[Title/Abstract] OR Intraoperative[Title/Abstract] OR Intra-operative[Title/Abstract] OR Respirat*[Title/Abstract] OR Breath*[Title/Abstract])) AND (Model*[Title/Abstract] OR Organ[Title/Abstract] OR *tissue[Title/Abstract])) AND (*rigid OR motion)) AND (deform*)) AND (Navigat* OR Guid* OR Regist* OR Align* OR Correlat*)	736
Google Scholar	(Intraoperative OR Intra-operative) AND (non-rigid OR nonrigid) AND (Deformation OR Motion) AND ( Registration OR Correlation)	495

Table 1: Summary of model-based methods for organ deformation modeling. (The studies with official implementation code are marked with an asterisk (\*).)

	Study	Year	Modeling methods	Organs
Geometry-based alignment	Smit et al. [115], Zhang et al. [12], Zhang et al. [114], Allan et al. [116]	2024, 2020, 2019, 2016	Coherent point drift	Liver, kidney, kidney, liver
	Zhang et al. [117], Sun et al. [118], Ma et al. [41]	2024, 2023, 2022	Non-rigid iterative closest points	Liver, soft tissues, liver
	Huang et al. [119]	2023	Hybrid mixture modeling	Liver/lung
	Xu et al. [120]	2023	Multi-constraint point set registration	Coronary artery
	Song et al. [121]	2023	Iterative Perspective-n-Point	Femoral artery
	Zhu et al. [122]*	2023	Manifold regularized modeling	Coronary artery
	Chen et al. [39]	2021	Multi-stage iterative closest points	Spine
	Chen et al. [123]	2021	Tissue properties-based modeling	Knee
	Yoon et al. [106]	2021	Hierarchical registration	Coronary artery
	Chen et al. [8]	2020	Two-level surface warping	Liver
	Garcia Guevara et al. [110]	2020	Adaptive compliance graph matching	Vascularized organs
	G�erard et al. [111]	2017	Image-based affine registration	Liver
	Maris and Fiorini [40], Lee et al. [124]	2017, 2010	Thin-plate spline registration	Breast, lung
	Nosrati et al. [112]	2015	Affine mapping transformation	Kidney
	Lange et al. [125]	2004	Multilevel B-splines	Liver
Biomechanical models	Yang et al. [33]	2024	BCs-free FE-model	Liver
	Ringel et al. [126]	2023	Regularized Kelvinlet model	Breast
	Richey et al. [100]	2022	FE-model	Breast
	Golse et al. [91], Peterlik et al. [11], Adagolodjo et al. [127], Collins et al. [128]	2021, 2018, 2018, 2017	Co-rotational FE-model	Liver
	Espinel et al. [129]	2020	Iterative closest point	Liver
	Haouchine et al. [95]	2020	FE-model	Brain
	Jobidon-Lavergne et al. [130]	2019	FE-model	Spine
	Adagolodjo et al. [131], Paulus et al. [113]	2017, 2017	Co-rotational FE-model	Liver/kidney
	Plantefeve et al. [67], Haouchine et al. [132]	2016, 2014	FE-model, beam elements	Liver
	Kong et al. [133], Wild et al. [134]	2017, 2016	FE-model	Kidney
	Haouchine et al. [135], Wu et al. [136], Haouchine et al. [137], Rucker et al. [79]	2016, 2014, 2013, 2013	FE-model	Liver
	Marques et al. [138], Haouchine et al. [139]	2015, 2012	Co-rotational FE-model	Liver
	Mohammadi et al. [140], Pheiffer et al. [141], Fan et al. [142]	2015, 2014, 2013	FE-model	Brain
	Conley et al. [143], Carter et al. [144]	2015, 2012	FE-model	Breast
	Khallaghi et al. [145]*, Fedorov et al. [146]*	2015, 2015	Gaussian mixture model & FE-model	Prostate
	Mountney et al. [147]	2014	Co-rotational FE-model	Abdominal organs
	Berkels et al. [148]	2013	FE-model	Abdominal and thoracic skin
	Haigron et al. [108]	2013	FE-model	Abdominal aortas
Li et al. [149]	2013	FE-model	Lung	
Zhuang et al. [99], Liu et al. [150], Bucki et al. [151], Wittek et al. [152]	2011, 2007, 2007, 2005	FE-model	Brain	
Dumpuri et al. [153], Cash et al. [154]	2010, 2007	FE-model	Liver	
Statistical models	Guezou-Philippe et al. [155]	2023	Statistical shape model	Pelvis
	Zhu et al. [107]	2021	Statistical shape model	Vascularized organs
	Li et al. [13, 89]	2019	Statistical motion model	Liver
	Zhou et al. [156]	2018	Statistical shape model	Liver
	Hu et al. [157]	2015	Kriging based model morphing	Bone
	Kadoury et al. [21]	2011	Statistical shape model	Spine
	Han et al. [158]	2009	Statistical deformation model	Kidney
Physics	Chen et al. [159], Liu et al. [160]	2024, 2021	Position-based dynamics modeling	Liver, soft tissues
	Reichard et al. [16], Suwelack et al. [35]*	2017, 2014	Physics-based shape matching	Liver/spleen, liver
	Costa [37]	2012	A quasi-static solution	Breast/liver
	Dagon et al. [36]	2008	A mass-spring based modeling	Liver

Table 2: Summary of data-driven and hybrid methods for organ deformation modeling. (The studies with official implementation code are marked with an asterisk (\*).)

	Study	Year	Modeling methods	Organs	
	<b>NetBiom</b>				
	Wang et al. [161]	2024	Spline-residual GCN + Biomechanical model	Liver	
	Labrunie et al. [49]	2023	CNN + 3D morphable models	Liver	
	Mendizabal et al. [162]*	2023	BANet2.0 + Biomechanical model	Liver	
	Tagliabue et al. [73]*	2021	BANet + Biomechanical model	Liver	
	<b>MultiDef</b>				
Hybrid algorithms	Ha et al. [163]	2024	CNN + Statistical shape model	Femur	
	Liebmann et al. [164]	2024	U-Net + Multi-stage iterative closest points	Spine	
	Zhang et al. [165]	2023	Vision Transformer + Thin-plate spline	Coronary artery	
	Shi et al. [10]	2022	U-Net + Generalized moving least-square algorithm	Liver	
	Haouchine et al. [97, 98]	2021, 2020	U-Net + Force-based shape-from-template formulation	Brain	
	Jia and Kyan [17]	2021	Point cloud occupancy network + Nonlinear optimization	Liver	
	Lei et al. [166]	2021	$\epsilon$ -support vector regression + Kriging algorithm	Liver/lung	
	Shakeri et al. [167]	2021	Deep variational autoencoder + Non-rigid optimal ICP	Prostate	
	Shi et al. [88]	2021	U-Net + Moving least-squares algorithm	Liver	
		<b>PhysDL</b>			
	Odot et al. [168]	2023	MLP + Optimal control	Liver	
	Min et al. [34]*	2023	Physics-informed DL	Prostate	
	Salehi and Giannacopoulos [169]*	2022	PhysGNN	Brain	
	<b>Machine learning approaches</b>				
Data-driven algorithms	El et al. [170]	2024	U-Net	Liver	
	Azampour et al. [171]*	2023	FlowNet3D	Spine	
	Young et al. [172]	2023	U-Net + Vision Transformer	Liver	
	Shao et al. [173]	2023	GCN + U-Net	Liver	
	Nakao et al. [70]*	2022	Image-to-graph convolutional network	Abdominal organ	
	Yamamoto et al. [174]	2021	Kernel regression	Lung	
	Pfeiffer et al. [31]*	2020	U-Net	Liver	
	Pfeiffer et al. [62]*	2019	U-Net	Liver	
	Mendizabal et al. [29]	2019	U-Net	Breast	
	Brunet et al. [61]	2019	U-Net	Liver	
		<b>Atlas-based modeling</b>			
	Heiselman et al. [55]	2018	Atlas-based modeling	Liver	
	Miga et al. [94]	2016	Atlas-based modeling	Brain	
	Chen et al. [54]	2013	Atlas-based modeling	Brain	
	Chen et al. [53]	2010	Atlas-based modeling	Brain	
Clements et al. [32]	2007	Atlas-based modeling	Liver		

Table 3: Comparison of different deformation modeling methods

Criteria	Model-based methods				Data-driven methods			Hybrid methods		
	Biom.	Phys.	Geom.	Stat.	Atlas	TML	DL	NetBiom	MultiDef	PhysDL
Accuracy	High	Medium	Low	High	Low	Medium	Low	Medium	Medium	Medium
Efficiency	Low	Medium	High	High	High	High	High	Medium	Low	High
Implementation	Low	High	High	Low	High	Low	High	High	High	High

Table 4: Public available datasets for organ deformation modeling

Datasets	Preoperative organ models	Deformed organ models	Intraoperative organ images	Validation targets	Organ	Subjects
Sparse Data Challenge [51]	✓	✓		✓	Phantom liver	1
Open-CAS LiverReg [35]	✓	✓		✓	Phantom liver	1
CALLR [175]	✓		✓	✓	Liver	4
DePoLL [176]	✓	✓	✓	✓	Porcine liver	1
Respiratory Motion [177]	✓	✓			Liver	4
3D-IRCADb-02 [178]	✓	✓			Abdominal organ	1
P2ILF (coming soon) [179]	✓		✓		Liver	11
C3VD [180]	✓		✓		Colon	1
Med-RAD [181]	✓	✓			Lung	3
Vascular Tree [120]	✓	✓			Coronary artery	16
Prostate-MRI-US-Biopsy [182]	✓	✓		✓	Prostate	642
Tissue Dissection [73]	✓	✓			Silicone phantoms	4

Table 5: Quantitative accuracy results reported in organ deformation modeling studies. (The studies with official implementation code are marked with an asterisk (\*).)

	Study	Year	Imaging modality	Experiments	Metrics	Results (unit: mm)
Hepatobiliary Surgery	Yang et al. [33]	2024	RGB-D images	Phantom	Average TRE	$3.14 \pm 1.34$
	Wang et al. [161]	2024	RGB-D images	In-silico	Average TRE	$3.23 \pm 0.76$
	Chen et al. [159]	2024	Structured light	Ex-vivo	TRE	1.24
	Smit et al. [115]	2024	US images	Clinical cases	Median TRE	6.90
	Mendizabal et al. [162]*	2023	RGB-D images	In-vivo	RMS TRE	0.87
	Young et al. [172]	2023	Stereo laparoscopy	In-silico	Average TRE	$4.70 \pm 0.50$
	Shao et al. [173]	2023	X-ray images	In-silico	95-percentile HD	$2.40 \pm 1.60$
	Labrunie et al. [49]	2023	Monocular laparoscopy	In-silico	Average TRE	$8.50 \pm 3.90$
	Huang et al. [119]	2023	RGB-D	Phantom	Average TRE	$8.58 \pm 0.84$
	Ma et al. [41]	2022	US images	1). Phantom; 2). Ex-vivo	Average TRE	1). $2.34 \pm 0.45$ ; 2). $4.49 \pm 1.88$ .
	Shi et al. [10]	2022	Optical trackers	In-vivo	TRE	2.50
	Golse et al. [91]	2021	RGB-D images	Ex-vivo	RMS TRE	7.90
	Jia and Kyan [17]	2021	RGB-D images	In-silico	Average TRE	$4.28 \pm 0.60$
	Espinel et al. [129]	2020	Monocular laparoscopy	Phantom	Average TRE	$5.53 \pm 1.41$
	Chen et al. [8]	2020	US images	Ex-vivo	Average TRE	$2.14 \pm 0.21$
	Pfeiffer et al. [31]*	2020	Stereo laparoscopy	In-silico	TRE	$TRE_{mean} 5.70$
	Li et al. [89]	2019	Optical trackers	In-vivo	Average TRE	$3.52 \pm 0.12$
	Li et al. [13]	2019	Optical trackers	In-vivo	Average TRE	$2.68 \pm 1.02$
	Brunet et al. [61]	2019	RGB-D images	Ex-vivo	TRE	$TRE_{mean} 2.92$
	Peterlík et al. [11]	2018	CBCT images	In-silico	TRE	$TRE_{mean} 3.80$
	Heiselman et al. [55]	2018	Spatial resampling	Phantom	Average TRE	$6.70 \pm 1.30$ .
	Collins et al. [128]	2017	Spatial resampling	Phantom	Average TRE	$5.30 \pm 0.50$
	Allan et al. [116]	2016	Stereo laparoscopy	Phantom	RMS TRE	2.89
	Haouchine et al. [132]	2014	Stereo endoscopy	Phantom	TRE	4.41
	Haouchine et al. [183]	2014	Stereo endoscopy	Ex-vivo	TRE	5.13
	Suwelack et al. [35]*	2014	RGB-D images	Phantom	TRE	8.70
	Plantefeve et al. [184]	2014	Stereo laparoscopy	In-vivo	Mean HD	0.60
	Haouchine et al. [185]	2013	Stereo endoscopy	Phantom	TRE	4.40
	Dumpuri et al. [153]	2010	RGB-D images	Clinical cases	Average TRE	$3.10 \pm 1.80$
	Cash et al. [154]	2007	RGB-D images	Phantom	RMS TRE	6.70
Cash et al. [186]	2005	Laser range scans	Phantom	RMS TRE	2.40	
Brain Surgery	Salehi and Giannacopoulos [169]*	2022	RGB-D images	In-silico	TRE	$0.31 \pm 0.69$
	Haouchine et al. [97]	2021	2D images	In-silico	TRE	$TRE_{max} 1.93$
	Haouchine et al. [95]	2020	2D images	In-silico	TRE	$TRE_{max} 2.00$
	Miga et al. [94]	2016	RGB-D images	Clinical cases	TRE	$TRE_{max} 4.00$
	Pheiffer et al. [141]	2014	Laser range scans	Clinical cases	Average TRE	$2.00 \pm 0.90$
	Zhuang et al. [99]	2011	Laser range scans	In-vivo	Average TRE	$1.62 \pm 0.22$
	Liu et al. [187]	2010	Laser range scans	In-vivo	TRE	1.20
	Liu et al. [150]	2007	Stereo-vision images	In-vivo	Surface distance	1.38
Wittek et al. [152]	2005	MRIs	In-silico	TRE	3.18.	



Table 6: Quantitative accuracy results reported in organ deformation modeling studies. (The studies with official implementation code are marked with an asterisk (\*).)

	Study	Year	Imaging modality	Experiments	Metrics	Results (unit: mm)
Vascular Surgery	Zhang et al. [165]	2023	DSA images	Clinical cases	Average HD	$1.73 \pm 0.62$
	Song et al. [121]	2023	DSA images	Clinical cases	Projected distance	3.74
	Zhu et al. [122]*	2023	DSA images	In-silico	Projected distance	0.34
	Yoon et al. [106]	2021	DSA images	In-silico	Projected distance	1.98
	Zhu et al. [107]	2021	DSA images	Clinical cases	Projected distance	$1.59 \pm 0.40$
	Garcia Guevara et al. [110]	2020	CBCT images	In-silico	TRE	4.20
	Garcia Guevara et al. [188]	2018	CBCT images	In-silico	Average TRE	$4.00 \pm 2.10$
	Gérard et al. [111]	2017	US images	In-silico	Average TRE	$3.90 \pm 1.10$
Haigron et al. [108]	2013	DSA images	Clinical cases	Average TRE	$2.90 \pm 0.50$	
Spine Surgery	Liebmann et al. [164]	2024	RGB-D images	Ex-vivo	Average TRE	$1.20 \pm 0.22$
	Azampour et al. [171]*	2023	US images	In-silico	Average TRE	$3.67 \pm 0.63$
	Chen et al. [39]	2021	Structured light	Ex-vivo	RMS TRE	$0.51 \pm 0.31$
	Jobidon-Lavergne et al. [130]	2019	CBCT images	Clinical cases	1). Surface distance; 2). Orientation error.	1). $1.50 \pm 1.20$ ; 2). $2.7 \pm 2.6^\circ$ .
	Kadoury et al. [21]	2011	CT images	Clinical cases	RMS TRE	$1.80 \pm 0.70$
	Rajamani et al. [189]	2007	US images	In-silico	Mean HD	1.76
Pulmonary Surgery	Huang et al. [119]	2023	RGB-D images	Clinical cases	Average TRE	$5.30 \pm 0.37$
	Yamamoto et al. [174]	2021	Sampled landmarks	In-silico	1). RMS TRE; 2). HD.	1). 2.74; 2). 6.11.
	Li et al. [149]	2013	CT images	Clinical cases	Average TRE	$1.30 \pm 0.97$
	Lee et al. [124]	2010	Laser range scans	Phantom	Average TRE	$2.32 \pm 0.23$
Breast Surgery, Orthopedic Surgery, Renal Surgery, Prostate Surgery	Ringel et al. [126]	2023	RGB-D images	Clinical cases	Average TRE	$3.00 \pm 1.10$
	Richey et al. [100]	2022	MRIs	In-vivo	Average TRE	$4.20 \pm 1.00$
	Mendizabal et al. [29]	2020	Optical trackers	Phantom	Average TRE	$4.21 \pm 1.01$
	Ha et al. [163]	2024	X-ray images	Clinical cases	Average HD	$4.43 \pm 0.85$
	Guezou-Philippe et al. [155]	2023	US images	In-vivo	Orientation error	$7.3 \pm 3.5^\circ$
	Chen et al. [123]	2021	Sampled landmarks	1). Phantom; 2). Ex-vivo.	Average TRE	1). $2.01 \pm 0.65$ ; 2). $2.97 \pm 0.79$ .
	Hu et al. [157]	2015	Spatial resampling	Phantom	RMS TRE	0.75.
	Zhang et al. [12]	2020	Stereo endoscopy	Phantom	Average TRE	$1.69 \pm 0.31$
	Zhang et al. [114]	2019	Stereo endoscopy	Phantom	RMS TRE	1.28
	Min et al. [34]*	2023	TRUS images	Clinical cases	Average TRE	$6.12 \pm 1.95$
	Shakeri et al. [167]	2021	TRUS images	In-silico	Average TRE	$3.90 \pm 1.40$
	Khallaghi et al. [145]*	2015	TRUS images	Clinical cases	Average TRE	$2.89 \pm 1.44$
Other Surgical Procedures	Nakao et al. [70]*	2022	X-ray images	In-silico	1). Surface distance; 2). HD.	1). $2.12 \pm 0.84$ ; 2). $10.27 \pm 4.02$ .
	Lei et al. [166]	2021	CT images	In-vivo	TRE	2.10
	Tagliabue et al. [73]*	2021	RGB-D images	Ex-vivo	RMS TRE	3.62
	Pfeiffer et al. [62]*	2019	RGB-D images	Phantom	TRE	$TRE_{mean} 5.10$
	Adagolodjo et al. [131]	2017	2D images	Phantom	TRE	2.20
	Paulus et al. [113]	2017	2D images	Phantom	Maximum HD	6.90